Ann. Henri Poincaré 14 (2013), 119–158

1424-0637/13/010119-40
published online May 19, 2012
DOI 10.1007/s00023-012-0184-x

Annales Henri Poincaré

A Matrix Model for the Topological String II: The Spectral Curve and Mirror Geometry

Bertrand Eynard, Amir-Kian Kashani-Poor and Olivier Marchal

Abstract. In a previous paper, we presented a matrix model reproducing the topological string partition function on an arbitrary given toric Calabi–Yau manifold. Here, we compute the spectral curve of our matrix model and thus provide a matrix model derivation of the large volume limit of the BKMP "remodeling the B-model" conjecture, the claim that Gromov–Witten invariants of any toric Calabi–Yau threefold coincide with the spectral invariants of its mirror curve.

1. Introduction

In a previous paper [1], we presented a matrix model $\mathcal{M}_{\mathfrak{X}}$ that computes the topological string partition function at large radius on an arbitrary toric Calabi–Yau manifold $\mathfrak{X}$,

$$Z_{\mathcal{M}_{\mathfrak{X}}} = Z_{\text{top}}(\mathfrak{X}).$$

The goal of this paper is to determine the corresponding spectral curve $\mathcal{S}(\mathcal{M}_{\mathfrak{X}})$. $\mathcal{M}_{\mathfrak{X}}$ is a chain of matrices matrix model with non-polynomial potential. An algorithm for determining the spectral curve of such a matrix model does not exist in the literature. Generalizing work of [2,3], we propose such an algorithm, and apply it to $\mathcal{M}_{\mathfrak{X}}$. A proof of the proposed algorithm will appear in a forthcoming publication (Eynard, B., Marchal, O.: Work in progress).

The interest in computing this curve is the following. A celebrated result in the theory of 1-matrix models is that their partition function can be recovered to all orders in an appropriate expansion parameter (the inverse size of the matrix $g_s = 1/N$) from their corresponding spectral curve $\mathcal{S}(\mathcal{M})$, using loop equations [4,5],

$$\ln Z_{\mathcal{M}} = \sum_{g=0}^{\infty} g_s^{2g-2} F_{\mathcal{M},g}. \tag{1.1}$$

A recursive algorithm to solve the loop equations and compute the coefficients $F_{\mathcal{M},g}$ of this expansion was developed in [6,7]. In [8], this recursive algorithm was promoted to the definition of symplectic invariants $F_g(\mathcal{S})$ of plane curves $\mathcal{S}$, with no reference to an underlying matrix model. When the plane curve is chosen as the spectral curve $\mathcal{S}_{\mathcal{M}}$ of a matrix model, these symplectic invariants reproduce the coefficients in the expansion (1.1),

$$F_{\mathcal{M},g} = F_g(\mathcal{S}_{\mathcal{M}}).$$

In our case, $\mathcal{M}$ is a chain of matrices matrix model. An explicit algorithm to compute $F_g(\mathcal{S}_{\mathcal{M}})$ by recursion was developed for this class of models, albeit with polynomial potentials, in [3].

The symplectic invariants $F_g(\mathcal{S})$ satisfy many properties reminiscent of the topological string free energies [9–11].[1] Against the backdrop of the link [12] between topological strings and Chern–Simons theory on the one hand and the link [13] between Chern–Simons theory and matrix models on the other [14], Bouchard, Klemm, Mariño, and Pasquetti (BKMP) [15], building on work of Mariño [16], were thus motivated to conjecture that they in fact coincide with the topological string free energies on a toric Calabi–Yau manifold $\mathfrak{X}$, provided that the plane curve $\mathcal{S}$ is chosen as the mirror curve $\mathcal{S}_{\mathfrak{X}}$ of $\mathfrak{X}$!

$$\text{BKMP conjecture:} \quad F_g(\mathcal{S}_{\mathfrak{X}}) \stackrel{!}{=} F_g^{\text{top}}(\mathfrak{X}).$$

BKMP successfully checked their claim for various examples, at least to low genus. The conjecture was subsequently studied in various works [17–26], providing additional support and proofs in numerous special cases.

The goal of this paper is to determine the spectral curve $\mathcal{S}_{\mathcal{M}_{\mathfrak{X}}}$ of our matrix model $\mathcal{M}_{\mathfrak{X}}$ and to compare it to the mirror curve $\mathcal{S}_{\mathfrak{X}}$ of $\mathfrak{X}$.

Recall that $\mathcal{M}_{\mathfrak{X}}$ is a chain of matrices matrix model with non-polynomial potential. The problem of determining the spectral curve of simple matrix models, such as the 1-matrix model, was solved long ago [4,27]. The problem becomes more difficult as the complexity of the matrix model increases. A procedure for determining the spectral curve for a chain of matrices with polynomial potentials exists in the literature [2,3], and is rather easy to apply to short chains of matrice, and when the potentials have low degree. It can be extended in a straightforward manner to potentials whose derivative is rational. Here, our matrix model $\mathcal{M}_{\mathfrak{X}}$ is a chain of matrices of arbitrary length, and the potentials are neither polynomials nor rationals—they involve quantum-Γ functions, hence an infinite number of poles. In this paper, we will re-formulate the procedure derived in [2,3] in terms of local properties of the potentials, such that is becomes applicable to $\mathcal{M}$. A short-coming of the approach of [2,3] is that

[1] The partition function $Z_{\text{top}}(\mathfrak{X})$ is defined via its expansion $\ln Z_{\text{top}}(\mathfrak{X}) = \sum_{g=0}^{\infty} g_s^{2g-2} F_g^{\text{top}}(\mathfrak{X})$, where the free energies $F_g^{\text{top}}(\mathfrak{X})$ are generating functions for Gromov–Witten invariants.

it does not necessarily yield a unique curve—intuitively, the spectral curve can be derived from an action principle, the procedure of [2,3] provides local extrema of the corresponding action, whereas the correct spectral curve lies at a global extremum (this intuition can be made precise in the 1-matrix case).

Following this route, we obtain a candidate spectral curve $\mathcal{S}_{\mathcal{M}_\mathfrak{X}}$ for our matrix model $\mathcal{M}_\mathfrak{X}$ which is distinguished by being of minimal genus and degree. We demonstrate that $\mathcal{S}_{\mathcal{M}_\mathfrak{X}}$ is indeed symplectically equivalent to the mirror curve $\mathcal{S}_\mathfrak{X}$ of $\mathfrak{X}$, and therefore, its symplectic invariants are the Gromov–Witten invariants of $\mathfrak{X}$, thus arriving at the statement of the BKMP conjecture. To elevate our result to a rigorous proof of this conjecture, we would need a formal proof that the curve we find, distinguished by minimality of genus and degree, indeed corresponds to a global extremum of the action principle.

Recall that in [1], we introduce the matrix model $\mathcal{M}_{\mathfrak{X}_0}$ for the topological string partition function on a toric Calabi–Yau geometry $\mathfrak{X}_0$ which we refer to as fiducial. Flops and limits in the Kähler cone relate $\mathfrak{X}_0$ to an arbitrary toric Calabi–Yau threefold. As we can follow the action of these operations on the partition function, we thus arrive at a matrix model for the topological string on any toric Calabi–Yau threefold. Here, we follow the analogous strategy, by first computing the spectral curve of the matrix model associated to $\mathfrak{X}_0$, and then studying the action of flops and limits on this curve.

The plan of the paper is as follows. As the BKMP conjecture identifies the Gromov–Witten invariants of a Calabi–Yau $\mathfrak{X}$ with the symplectic invariants of its mirror curve $\mathcal{S}_\mathfrak{X}$, we begin in Sect. 2 with a brief review of mirror symmetry in the case of toric Calabi–Yau manifolds. We introduce here the fiducial geometry $\mathfrak{X}_0$ and its mirror curve $\mathcal{S}_{\mathfrak{X}_0}$. The matrix model $\mathcal{M}_{\mathfrak{X}_0}$, as derived in [1], is summarized in Sect. 3 and Appendix A. We review general aspects of this class of matrix models in Sect. 4, and then present the generalization of the results of [2,3] for finding the associated spectral curves. In Sect. 5, we determine a curve which satisfies all specifications outlined in Sect. 4, and demonstrate that it coincides, up to symplectic transformations, with the B-model mirror of the fiducial geometry. As these specifications do not necessarily specify the spectral curve uniquely, we provide additional consistency arguments for our proposal for the spectral curve in Sect. 5.5. Flops and limits in the Kähler cone relate the fiducial to an arbitrary toric Calabi–Yau manifold. Following the action of these operations on both sides of the conjecture in Sect. 6 completes the argument yielding the BKMP conjecture for arbitrary toric Calabi–Yau manifolds in the large radius limit. We conclude by discussing possible avenues along which this work can be extended.

2. The Fiducial Geometry and its Mirror

2.1. The Fiducial Geometry

In [1], we derived a matrix model reproducing the topological string partition function on the toric Calabi–Yau geometry $\mathfrak{X}_0$ whose toric fan is depicted in Fig. 1. We refer to $\mathfrak{X}_0$ as our fiducial geometry; we will obtain the partition

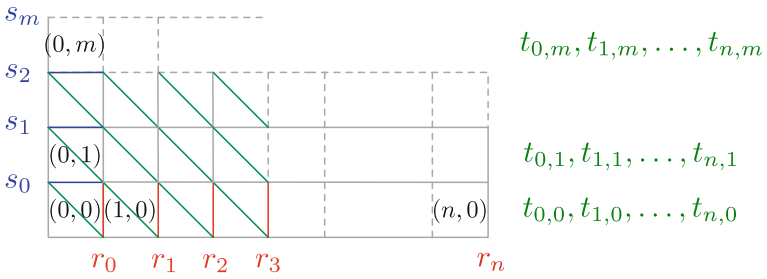

FIGURE 1. Fiducial geometry $\mathfrak{X}_0$ with boxes numbered and choice of basis of $H_2(\mathfrak{X}_0, \mathbb{Z})$

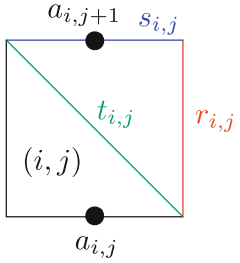

FIGURE 2. Labeling curve classes, and introducing a-parameters

function on an arbitrary toric Calabi–Yau manifolds by considering flops and limits of $\mathfrak{X}_0$.

We have indicated a basis of $H_2(\mathfrak{X}_0, \mathbb{Z})$ in Fig. 1. Applying the labeling scheme introduced in Fig. 2, the curve classes of our geometry are expressed in this basis as follows,

$$r_{i,j} = r_i + \sum_{k=1}^{j} (t_{i+1,k-1} - t_{i,k})$$

$$s_{i,j} = s_j + \sum_{k=1}^{i} (t_{k-1,j+1} - t_{k,j}).$$

It proves convenient to express these classes as differences of what we will refer to as a-parameters [1], defined via

$$t_{i,j} = g_s(a_{i,j} - a_{i,j+1}), \qquad r_{i,j} = g_s(a_{i,j+1} - a_{i+1,j}). \tag{2.1}$$

$s_{i,j}$ classes are not related to a-parameters.

2.2. The Mirror of the Fiducial Geometry

The Hori–Vafa prescription [28] allows us to assign a mirror curve to a toric Calabi–Yau manifold. Each torically invariant divisor, corresponding to a 1-cone $\rho \in \Sigma(1)$, is mapped to a $\mathbb{C}^*$ variable e^{-Y_ρ}. These are constrained by the equation

$$\sum_{\rho\in\Sigma(1)} e^{-Y_\rho} = 0.$$

Relations between the 1-cones, as captured by the lattice Λ_h introduced in section 2.1 of [1], map to relations between these variables: for $\sigma \in \Sigma(2)$,

$$\sum_{\rho\in\Sigma(1)} \lambda_\rho(\sigma) Y_\rho = W_\sigma. \tag{2.2}$$

The W_σ are complex structure parameters of the mirror geometry, related to the Kähler parameters $w_\sigma = r_{i,j}, s_{i,j}, t_{i,j}, \ldots$ introduced in the previous subsection via the mirror map, as we will explain in the next subsection.

The Hori–Vafa prescription gives rise to the following mirror curve $\mathcal{C}_{\mathfrak{X}_0}$ of our fiducial geometry $\mathfrak{X}_0$,

$$\sum_{i=0}^{n+1}\sum_{j=0}^{m+1} x_{i,j} = 0. \tag{2.3}$$

We have here labeled the 1-cones by coordinates (i, j), beginning with $(0, 0)$ for the cone $(0, 0, 1)$ in the bottom left corner of box $(0, 0)$ as labeled in Fig. 1, and introduced the notation

$$x_{i,j} = e^{-Y_{i,j}}. \tag{2.4}$$

Eliminating dependent variables by invoking (2.2) yields an homogeneous equation of the form

$$\sum_{i=0}^{n+1}\sum_{j=0}^{m+1} c_{i,j} z_{i,j} = 0. \tag{2.5}$$

Here,

$$z_{i,j} = x_0^{1-i-j} x_1^i x_2^j,$$

where we have defined

$$x_0 = x_{0,0}, \quad x_1 = x_{1,0}, \quad x_2 = x_{0,1}.$$

$(x_0 : x_1 : x_2)$ define homogeneous coordinates on $\mathbb{CP}^2$. Due to the relation (2.4) between the coordinates x_i and the physical variables Y_i, any point on the curve with a vanishing homogeneous coordinate corresponds to a puncture. The form of the equation is independent of the choice of triangulation of the toric diagram. What does depend on this choice are the coefficients $c_{i,j}$. It is not hard to write these down for the fiducial geometry $\mathfrak{X}_0$ with the choice of basis for $H_2(\mathfrak{X}_0, \mathbb{Z})$ indicated in Fig. 1. Explicitly, the relations between the coordinates of the mirror curve (2.3) are

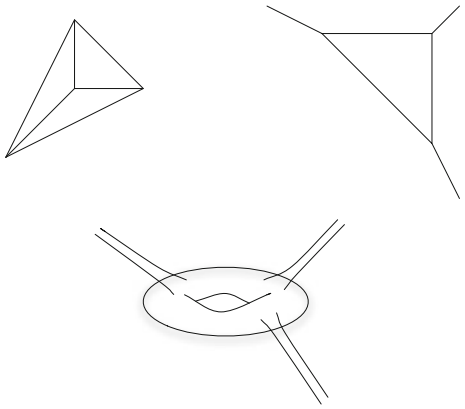

FIGURE 3. Example of the thickening prescription: depicted are the fan for $\mathcal{O}(-3) \to \mathbb{P}^2$, the corresponding web diagram, and the mirror curve obtained via the thickening prescription

$$\begin{aligned} x_{i,0} &= \frac{x_{i-1,0}x_{i-1,1}}{x_{i-2,1}} e^{R_{i-2}} \\ x_{0,j} &= \frac{x_{0,j-1}x_{1,j-1}}{x_{1,j-2}} e^{S_{j-2}} \\ x_{i,j} &= \frac{x_{i-1,j}x_{i,j-1}}{x_{i-1,j-1}} e^{T_{i-1,j-1}}. \end{aligned} \tag{2.6}$$

Solving in terms of x_0, x_1, x_2 yields the coefficients $c_{0,0} = c_{0,1} = c_{1,0} = 1$,

$$\begin{aligned} c_{i,0} &= \exp\left[\sum_{k=1}^{i-1}(i-k)(R_{k-1} + T_{k-1,0})\right], \\ c_{0,j} &= \exp\left[\sum_{l=1}^{j-1}(j-l)(S_{l-1} + T_{0,l-1})\right], \end{aligned}$$

and for $i, j > 0$

$$\begin{aligned} c_{i,j} = \exp\Bigg[&(i+j-1)T_{0,0} + \sum_{k=1}^{i-1}(i-k)(R_{k-1} + T_{k,0}) \\ &+ \sum_{l=1}^{j-1}(j-l)(S_{l-1} + T_{0,l}) + \sum_{k=1}^{i-1}\sum_{l=1}^{j-1} T_{k,l}\Bigg]. \end{aligned}$$

Note that the number of coefficients $c_{i,j}$, up to an overall rescaling, is equal to the number of independent curve classes $r_i, s_j, t_{i,j}$.

In [29], the thickening prescription was put forth for determining the genus and number of punctures of the mirror curve: one is to thicken the web diagram of the original geometry to obtain the Riemann surface of the mirror geometry. The procedure is illustrated in Fig. 3. We will now verify this procedure by studying the curve (2.5) explicitly.

Let us consider the curve (2.5) for a single strip (i.e. $n = 0$) of length $m + 1$,

$$x_0^{m+2} + x_0^{m+1}x_1 + x_0^{m+1}x_2 + c_{1,1}x_0^m x_1 x_2 + c_{2,0}x_0^m x_1^2 + c_{2,1}x_0^{m-1}x_1^2 x_2 + c_{3,0}x_0^{m-1}x_1^3 + \cdots + c_{m+1,0}x_0 x_1^{m+1} + c_{m+1,1}x_1^{m+1}x_2 = 0. \tag{2.7}$$

Note that the equation is of degree $d = m + 2$, but the point $(0 : 0 : 1)$ is an $m + 1$-tuple point. By choosing the coefficients to be generic, we can arrange for this singular point to be ordinary. The genus formula then yields

$$\mathfrak{g} = \frac{(d-1)(d-2)}{2} - \frac{m(m+1)}{2} = 0.$$

Points on the curve with a vanishing homogeneous coordinate correspond to punctures. The punctures on the curve (2.7) thus lie at

$$\begin{aligned}(0:0:1) &: m+1\\ (0:1:0) &: 1\\ (1:x_1^i:0) &: m+1\\ (1:0:-1) &: 1,\end{aligned}$$

where $x_1^i, i = 1, \ldots, m + 1$, are the solutions of the equation

$$1 + x_1 + \sum_{j=1}^{m} d_i x_1^{i+1} = 0.$$

Note that we reproduce the $2m + 4$ punctures expected from the thickening prescription of the toric diagram.

For the general case parametrized by (m, n), the degree of the curve is $d = m + n + 2$, and we have an ordinary $m + 1$-tuple point at $(0 : 0 : 1)$ and an ordinary $n + 1$-tuple point at $(0 : 1 : 0)$. The genus formula now yields

$$\mathfrak{g} = \frac{(m+n)(m+n+1)}{2} - \frac{m(m+1)}{2} - \frac{n(n+1)}{2} = mn.$$

The punctures lie at

$$\begin{aligned}(0:0:1) &: m+1\\ (0:1:0) &: n+1\\ (1:x_1^i:0) &: m+1\\ (1:0:x_2^j) &: n+1,\end{aligned}$$

with x_1^i the roots of $\sum_{i=0}^{m+1} c_{i,0}x_1^i = 0$ and x_2^j the roots of $\sum_{j=0}^{n+1} c_{0,j}x_2^j = 0$. Again, we see that we reproduce the thickening prescription.

2.3. The Mirror Map

Above, we have distinguished between Kähler (A-model) parameters w_σ and complex structure (B-model) parameters W_σ. At large radius/complex structure, these are identified between mirror pairs, but this identification is corrected by the so-called mirror map,[2]

$$W_\sigma = w_\sigma + \mathcal{O}(e^{-w_\sigma}). \tag{2.8}$$

The exponentials of the parameters W_σ appear as coefficients in the equation defining the mirror curve. They are global coordinates on the complex structure moduli space of the mirror curve. To compare expressions obtained in the A-model to those obtained in the B-model, all expressions are conventionally expressed in terms of flat coordinates w_σ.[3] On the A-model side, these coordinates enter (in exponentiated form denoted generically as $Q_{\alpha,\beta}$ below) in the definition of the topological vertex. On the B-model side, they arise as the appropriate periods of a meromorphic one-form λ, defined in terms of the affine variables $x = \frac{x_1}{x_0}, y = \frac{x_2}{x_0}$ in the patch $x_0 \neq 0$ of the curve (2.5) as

$$\lambda = \log y \frac{\mathrm{d}x}{x}.$$

By calculating these periods as a function of the coefficients defining the mirror curve, we obtain the mirror map (2.8) [30].

Note that the starting point of our considerations was the expression of the topological string partition function obtained from the topological vertex, hence as a function of the coordinates w_σ. An algebraic equation for the spectral curve will depend explicitly on the coordinates W_σ. Our goal of specifying the spectral curve of our matrix model hence ostensibly requires solving the

[2] One could take exception to this nomenclature, arguing that the parameters W_σ are the geometric parameters on both sides of the mirror, and refer to the w_σ as the instanton or quantum corrected parameters. In such conventions, the curve classes in the various toric diagrams should be labeled by upper case letters.

[3] The coordinates w_σ are not globally defined functions on the complex structure moduli space. In the slightly clearer compact setting, this is due to the fact that the symplectic basis $\{\alpha_A, \beta^A\}$ of $H^3(\mathfrak{X}, \mathbb{Z})$ in which we expand Ω (the compact analogue of the meromorphic 1-form λ introduced above) such that the coefficients of α_A furnish our (local) coordinate system of the complex structure moduli space, undergo monodromy when transported around a singularity in moduli space. A good choice of coordinates in the vicinity of a singular divisor D hence involves a choice of basis forms that are invariant under monodromy around that divisor. Note that the symplectic basis makes no reference to complex structure, one might hence be led to believe that a global choice (i.e. one valid for any choice of complex structure) should be possible. This is not so. We consider the family $\pi : \mathcal{X} \to \mathcal{S}$, with $\mathcal{S}$ the complex structure moduli space. The fiber over each point $w \in \mathcal{S}, \pi^{-1}w = X_w$, is the Calabi–Yau manifold with the respective complex structure. $H^n(X_w, \mathbb{C})$ fit together to form a vector bundle $\mathcal{F}_0$ over $\mathcal{S}$, with a canonical flat connection, the Gauss–Manin connection. Using this connection, we can parallel transport a symplectic basis of $H^3(X_w, \mathbb{C})$ along a curve in $\mathcal{S}$. As $\mathcal{S}$ is not generically simply connected (due to the existence of degeneration points of the geometry), this transport may exhibit monodromy. Note that Ω can be defined as the section of a sheaf in the Hodge filtration of H^3 which extends to the singular divisor, hence is single valued. The monodromy in our choice of flat coordinates is therefore entirely due to the choice of symplectic basis.

mirror map. In Sect. 5.3, we will see how the matrix model analysis elegantly allows us to bypass this difficulty.

3. Our Matrix Model

We derived a chain of matrices matrix model that reproduces the topological string partition function on $\mathfrak{X}_0$ in [1]. For $\mathfrak{X}_0$ of size $(n+1)\times(m+1)$, as depicted in Fig. 1, it is given by

$$\begin{aligned} Z_{\mathrm{MM}}(\vec{Q}, g_s, \vec{\alpha}_{m+1}, \vec{\alpha}_0^T) = {} & \Delta(X(\vec{\alpha}_{m+1}))\Delta(X(\vec{\alpha}_0)) \\ & \times \prod_{i=0}^{m+1} \int_{H_N(\Gamma_i)} dM_i \prod_{i=1}^{m+1} \int_{H_N(\mathbb{R}_+)} dR_i \\ & \times \prod_{i=1}^{m} e^{\frac{-1}{g_s}\mathrm{tr}\left[V_{\vec{\alpha}_i}(M_i) - V_{\vec{\alpha}_{i-1}}(M_i)\right]} \\ & \times \prod_{i=1}^{m} e^{\frac{-1}{g_s}\mathrm{tr}\left[V_{\vec{\alpha}_{i-1}}(M_{i-1}) - V_{\vec{\alpha}_i}(M_{i-1})\right]} \\ & \times \prod_{i=1}^{m+1} e^{\frac{1}{g_s}\mathrm{tr}\,(M_i - M_{i-1})R_i} \prod_{i=1}^{m} e^{(S_i + \frac{i\pi}{g_s})\mathrm{tr}\,\ln M_i} \\ & \times e^{\mathrm{tr}\,\ln f_0(M_0)} e^{\mathrm{tr}\,\ln f_{m+1}(M_{m+1})} \prod_{i=1}^{m} e^{\mathrm{tr}\,\ln f_i(M_i)}. \end{aligned} \tag{3.1}$$

All matrices are taken of size $N = (n+1)d$, with d a cut-off that we explained below. We give the explicit expressions for the various functions entering in this definition in Appendix A. Here, we briefly explain some of its general features.

The matrix model (3.1) is designed to reproduce the topological string partition function on the toric Calabi–Yau manifold $\mathfrak{X}_0$ as computed using the topological vertex [31]. Recall that in this formalism, the dual web diagram to the toric diagram underlying the geometry is decomposed into trivalent vertices. Each such vertex contributes a factor $C(\alpha_i, \alpha_j, \alpha_k)$ [31], where α_i denote Young tableaux (partitions) of arbitrary size, one associated to each leg of the vertex. Legs of different vertices are glued by matching these Young tableaux and summing over them with appropriate weight.

Aside from the coupling constant g_s and Kähler parameters $g_s a_{i,j}$ and $g_s S_i$ of the geometry, denoted collectively as $\vec{Q} = (q^{a_{i,j}}, q^{S_i})$, the matrix model (3.1) depends on partitions $\vec{\alpha}_0, \vec{\alpha}_{m+1}$ associated to the outer legs of the web diagram, which we choose to be trivial in this paper. The two classes of integrals dR_i and dM_i correspond to the two steps in which the topological string partition function on the fiducial geometry $\mathfrak{X}_0$ can be evaluated: first, the geometry can be decomposed into $m+1$ horizontal strips, with partitions $\alpha_{j,i+1}$ and $\alpha_{j,i}$ associated to the upper and lower outer legs of the associated strip web diagram. $j = 0, \ldots, n$ counts the boxes in Fig. 1 in the horizontal direction,

$i = 0, \dots, m+1$ is essentially the strip index. Each such strip has a dR_i integration associated to it. The partition function on such strips was calculated in [32]. Following [20], we introduce two matrices M_i, M_{i+1} per strip. Their eigenvalues encode the partitions $\alpha_{j,i}$ and $\alpha_{j,i+1}$ for all j. To work with finite size matrices, we introduce a cut-off d on the number of rows of the Young tableaux we sum over. As we argue in Sect. 5.2.1, our matrix model depends on d only non-perturbatively. The strip partition function is essentially given by the Cauchy determinant of the two matrices M_i, M_{i+1} [1], and the dR_i integrals are the associated Laplace transforms. Gluing the strips together involves summing over the partitions $\alpha_{j,i}$. This step is implemented by the dM_i integrations. To obtain a discrete sum over partitions from integration, we introduce functions $f_i(M_i)$ with integrally spaced poles. Integrating M_i along appropriate contours then yields the sum over partitions as a sum over residues, the potentials $V_{\vec{a}_i}$ chosen to provide the proper weight per partition.

4. Generalities on Solving Matrix Models

4.1. Introduction to the Topological Expansion of Chain of Matrices

Chain of matrices matrix models have been extensively studied (see Mehta's book [33] and the review article [34]), and the computation of their topological expansion was performed recently in [2,3].

The solution provided in [3] is based on the computation of the spectral curve $\mathcal{S}_{\mathcal{M}}$ of the matrix model. The spectral curve is defined to be the planar[4] limit of the expectation value of the resolvent of the first matrix of the chain.

In [2,3], only the case of polynomial potentials is considered, and the spectral curve is shown to be algebraic. It is easy to see that the results of [2,3] can be extended to the case of potentials whose derivatives are rational functions. An algebraic function is determined by a polynomial equation, and thus one has to determine the coefficients of this polynomial equation, i.e. a finite number of coefficients. In [2,3], these coefficients are determined by studying the asymptotic behavior of the solutions of the algebraic equation, supplemented with information coming from period integrals.

Our matrix model $\mathcal{M}$, the potentials contain logs of quantum Gamma functions (g-functions see eq. A.4). Their derivatives have an infinite number of poles, and thus the spectral curve is not algebraic. If we consider an expansion of the spectral curve in powers of q however, it will be a rational function at each finite order in q. Our strategy will hence be to take a limit of the recipe of [2,3]. To this end, in Sect. 4.2.2 below, we re-write the recipe of [2,3] in terms of local properties, such that it becomes independent of the number

[4] For matrix models with N-independent polynomial potentials whose g_s dependence is given by an overall prefactor, the planar limit coincides with the large N limit, but this correspondence can fail if the potential or the integration contours have a non-trivial N or g_s dependence. The planar limit is defined by keeping only planar graphs in the Feynman graph perturbative expansion around an extremum of the potential. However, it is helpful to have in mind the intuitive picture that the planar limit is similar to a large N limit.

or degrees of poles. That this indeed yields the correct generalization of [2,3] will be demonstrated in (Eynard, B., Marchal, O.: Work in progress).

Having found the spectral curve $\mathcal{S}_{\mathcal{M}}$ of the matrix model, we will compute its symplectic invariants $F_g(\mathcal{S}_{\mathcal{M}})$.

As mentioned in the introduction, symplectic invariants $F_g(\mathcal{S})$ can be computed for any analytical plane curve $\mathcal{S}$, and thus in particular for $\mathcal{S} = \mathcal{S}_{\mathcal{M}}$. For a general $\mathcal{S}$ they were first introduced in [8]. Their definition is algebraic and involves computation of residues at branch points of $\mathcal{S}$. We recall the definition below in Sect. 4.3.

4.2. Definition of the General Chain of Matrices

We consider chain of matrices matrix models of the form

$$Z = \int_{\mathcal{E}} dM_1 \dots dM_L e^{-\frac{1}{g_s}\mathrm{Tr}\sum_{i=1}^{L} V_i(M_i)} e^{\frac{1}{g_s}\mathrm{Tr}\sum_{i=1}^{L-1} c_i M_i M_{i+1}}. \tag{4.1}$$

Note that aside from the potentials $V_i(M_i)$, the only interactions are between nearest neighbors, whence the name "chain of matrices." Chain of matrices matrix models can be solved when the interaction terms between different matrices are of the form $\mathrm{Tr}\, M_i M_{i+1}$, as is the case here.

$\mathcal{E}$ can be any ensemble of L normal matrices of size $N \times N$, i.e. a submanifold of $\mathbb{C}^{LN^2}$ of real dimension LN^2, such that the integral is convergent. $\mathcal{E}$ can be many things; for a chain of matrices model, it is characterized by the contours on which eigenvalues of the various normal matrices are integrated (see [35] for the 2-matrix model case). For (4.1) to have a topological expansion, $\mathcal{E}$ must be a so-called steepest descent ensemble (see [36], section 5.5). For a generic ensemble $\mathcal{E}$ which would not be steepest descent, $\ln Z$ would be an oscillating function of $1/g_s$, and no small g_s expansion would exist, see [37].

The matrix model introduced in [1] and reproduced in Sect. 3 was defined to reproduce the topological string partition function, which is defined as a formal series in g_s, and therefore has a topological expansion by construction.

An ensemble $\mathcal{E}$ is characterized by filling fractions $n_{j,i}$,

$$\mathcal{E} = \prod_{i=1}^{L} \mathcal{E}_i \quad , \quad \mathcal{E}_i = H_N(\gamma_{1,i}^{n_{1,i}} \times \gamma_{2,i}^{n_{2,i}} \times \dots \times \gamma_{k_i,i}^{n_{k_i,i}}), \tag{4.2}$$

where $H_N(\gamma_1^{n_1} \times \dots \times \gamma_k^{n_k})$ is the set of normal matrices with n_1 eigenvalues on path γ_1, n_2 eigenvalues on path $\gamma_2, \dots, n_k$ eigenvalues on path γ_k.

As the filling fractions $n_{j,i}$ must satisfy the relation

$$\sum_{j=1}^{k_i} n_{j,i} = N$$

for all i, only $\sum_i (k_i - 1)$ of them are independent.

We also allow some paths $\gamma_{j,i}$ to have endpoints where $e^{-\mathrm{Tr}\sum_{i=1}^{L}(V_i(M_i) - M_i M_{i+1})} \neq 0$—indeed, in our matrix model, the matrices R_i are integrated on $H(\mathbb{R}_+^N)$.

4.2.1. The Resolvent. The spectral curve encodes all $W_i(x)$, the planar limits (see Footnote 4) of the resolvents of the matrices M_i,

$$W_i(x) = g_s \left\langle \mathrm{tr} \frac{1}{x - M_i} \right\rangle_{\mathrm{planar}},$$

see equation (4.5) below. The respective W_i can be expressed as the Stieljes transform

$$W_i(x) = \int \frac{\rho_i(x')\mathrm{d}x'}{x - x'}$$

of the planar expectation value of the eigenvalue density $\rho_i(x)$ of the matrix M_i,

$$\rho_i(x) = g_s \left\langle \mathrm{tr}\, \delta(x - M_i) \right\rangle_{\mathrm{planar}}.$$

By general properties of Stieljes transforms, singularities of $W_i(x)$ coincide with the support of the distribution $\rho_i(x)\mathrm{d}x$:

- Simple poles of $W_i(x)$ correspond to delta distributions i.e. isolated eigenvalues.
- Multiple poles correspond to higher derivatives of delta distributions.
- Cuts correspond to finite densities, the density being the discontinuity of $W_i(x)$ along the cut,

$$\rho_i(x) = \frac{1}{2i\pi}(W_i(x - i0) - W_i(x + i0)). \tag{4.3}$$

In particular, cuts emerging from algebraic singularities (generically square root singularities) correspond to densities vanishing algebraically (generically as square roots) at the endpoints of the cut. Cuts emerging from logarithmic singularities correspond to constant densities.

4.2.2. The Spectral Curve of the General Chain of Matrices. For polynomial potentials V_i, [2,3] derive a set of rules which allow the determination of the spectral curve. It is algebraic of degree $\prod_i \deg V_i'$ in this case. It is straightforward, following for instance the methods used in [38], to see that the rules of [2,3] apply to all potentials whose derivatives V_i' are rational. The spectral curve remains algebraic, of degree $\prod_i \deg V_i'$, with $\deg V_i'$ the sum of degrees of all poles of V_i'. For our purposes, we require yet more generality: the derivatives of our potentials V_i' involve quantum digamma functions $\psi_q(x)$ (see Appendix A):

$$\psi_q(x) = \sum_{n=1}^{\infty} \frac{q^n}{x - q^n}.$$

As V_i' are rational functions in a q expansion *to any given order*, we may however apply the rules of [2,3] perturbatively in powers of q (recall that our matrix model was defined to reproduce the topological vertex formula order by order as a power series in q).

Hence, straightforward generalizations of the results of [2,3] together with one assumption which we outline below under rule 2 yield the following procedure to determine the spectral curve for our matrix model with non-polynomial potentials V_i and V_i' non-rational. Following each rule, we comment in italics on the relation to the prescription derived in [2,3].

1. We will look for a Riemann surface $\mathcal{C}$ and $L+2$ analytical functions on $\mathcal{C}$,

$$x_0(z), x_1(z), x_2(z), \ldots, x_L(z), x_{L+1}(z) : \mathcal{C} \to \mathbb{CP}^1,$$

satisfying the functional relations

$$\forall i = 1, \ldots, L \qquad c_{i-1}x_{i-1}(z) + c_{i+1}x_{i+1}(z) = V_i'(x_i(z)). \tag{4.4}$$

Recall that the c_i are the coefficients of the interaction potentials in (4.1). We have set $c_0 = c_L = 1$. There will be a minimal genus for $\mathcal{C}$ consistent with these and the following conditions on the x_i.

For each $i = 1, \ldots, L$, the Riemann surface $\mathcal{C}$ can be realized as a branched covering of $\mathbb{CP}^1$ by the projection $x_i : \mathcal{C} \to \mathbb{CP}^1$. A choice of sheets for a branched covering is not unique: the choice consists in the set of cuts connecting branch points (recall that these are points at which $\mathrm{d}x_i(z) = 0$). We will impose conditions on this choice in step 4.

Rule 1 is identical to the rule written in [2,3].

2. If some path $\gamma_{j,i}$ has an endpoint a (called "hard edge" in the matrix model literature, see [38]), then choose a pre-image $a_i \in x_i^{-1}(a)$ and require

$$\mathrm{d}x_i(a_i) = 0 \quad \text{and} \quad x_{i-1}(z) \text{ has a simple pole at } z = a_i.$$

The topological recursion is proved in [3] *for chains of arbitrary length L without hard edges, but it is proved in the case $L = 1$ with hard edges in* [39]*, and the spectral curve with hard edges is found for $L = 2$ in* [38]*. It appears straightforward to extend these results to arbitrary length L. We plan to prove this in a future work. Here, we shall assume that this extension is possible.*

3. The functions $x_i(z)$ are to be holomorphic away from the points a_i as well as the points $z \in \mathcal{C}$ at which $V_{i-1}'(x_{i-1}(z))$ or $V_{i+1}'(x_{i+1}(z))$ is singular.

[2,3] *require that x_i is a meromorphic function with only two poles of prescribed degrees. One can see that those two poles are indeed the only places where $V_{i-1}'(x_{i-1}(z))$ or $V_{i+1}'(x_{i+1}(z))$ is singular. We have here generalized this rule as appropriate for non-polynomial potentials. The degrees of the poles in* [2,3] *are in fact a consequence of rule 1.*

4. Choose some contours $\widehat{\mathcal{A}}_{j,i}, j = 1, \ldots, k_i$ in $\mathbb{CP}^1$, such that each $\widehat{\mathcal{A}}_{j,i}$ surrounds all points of the contour $\gamma_{j,i}$ (related to the matrix ensemble $\mathcal{E}_i$ defined in (4.2)) in the clockwise direction and intersects no other contour $\gamma_{j',i}$. Recall that k_i denotes the number of cuts of the ith matrix, as implicitly defined in (4.2). Then choose a connected component $\mathcal{A}_{j,i} \subset \mathcal{C}$ of the pre-image of the contour $\widehat{\mathcal{A}}_{j,i}$ under x_i,

$$\mathcal{A}_{j,i} \subset x_i^{-1}(\widehat{\mathcal{A}}_{j,i}),$$

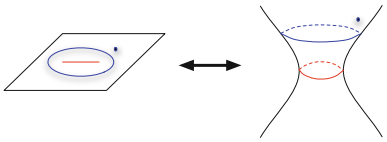

FIGURE 4. The integration contour $\widehat{\mathcal{A}}_{j,i}$ on the x-plane, and its image $\mathcal{A}_{j,i}$ on $\mathcal{C}$

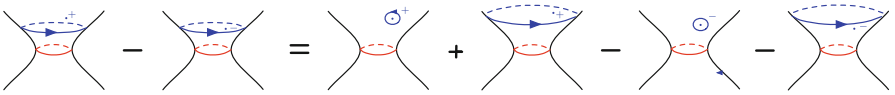

FIGURE 5. The preimage of the points x_+ and x_- of (4.6) are depicted as *dots* in the above diagram, $\widehat{\mathcal{A}}_{j,i}$ is given by the *blue contour*, and the preimage of the cut is drawn in *red*. To take the limit $x_+ \to x_-$, one must first shift the contours. The second and fourth term on the RHS of the above diagrammatic equation then cancel, yielding the RHS of (4.6) (color figure online)

Then, for $x \in \mathbb{CP}^1$ not enclosed in the contours $\widehat{\mathcal{A}}_{j,i}, j = 1, \ldots, k_i$, define the function

$$W_i(x) = \frac{c_{i-1}}{2i\pi} \sum_{j=1}^{k_i} \oint_{\mathcal{A}_{j,i}} \frac{x_{i-1}(z)\mathrm{d}x_i(z)}{x - x_i(z)}. \tag{4.5}$$

Generalizing [2] to non-polynomial potentials, we claim that a choice of $\mathcal{A}_{j,i}$ exists such that $W_i(x)$ is the planar limit of the resolvent of the matrix M_i. In the following, it is this choice that will be referred to as $\mathcal{A}_{j,i}$. It follows as a condition on the choice of branched covering that $\mathcal{A}_{j,i}$ and a_i must lie on the same sheet of x_i.

$W_i(x)$ depends only on the homology class of $\mathcal{A}_{j,i}$ on $\mathcal{C}$. Notice that not all $\mathcal{A}_{j,i}$ will be homologically independent on $\mathcal{C}$. $W_i(x)$ thus defined is analytical in $\mathbb{CP}^1$ for x outside of $\widehat{\mathcal{A}}_{j,i}$, but since one can homotopically deform the contours $\mathcal{A}_{j,i}$, it is in fact analytical outside of the cuts surrounded by the contours $\widehat{\mathcal{A}}_{j,i}$.

Rule 4 was mentioned as remark eq. 5.23 in [2].

5. In accord with (4.3), we consider the discontinuity of $W_i(x)$ along the jth cut. It is given by

$$\begin{aligned} \operatorname*{Disc}_j W_i(x) &= \frac{1}{2\pi i} \left(W_i(x_+) - W_i(x_-) \right) \\ &= \frac{1}{2\pi i} c_{i-1} \operatorname*{Disc}_j x_{i-1}, \end{aligned} \tag{4.6}$$

as we explain in Figs. 4 and 5.

The definition (4.2) of the matrix ensemble $\mathcal{E}_i$ is the condition that there are $n_{j,i}$ eigenvalues of M_i on the contour $\gamma_{j,i}$, hence corresponds to imposing the filling fraction conditions

$$\frac{1}{2\pi i}\oint_{\mathcal{A}_{j,i}} c_{i-1}x_{i-1}\mathrm{d}x_i = g_s n_{j,i}$$

for $i = 1, \ldots, L, j = 1, \ldots, k_i$.

Rule 5 can be found in [2, 3].

The spectral curve is defined as the data of the Riemann surface $\mathcal{C}$, and the two functions $x_1(z)$ and $x_2(z)$,

$$\boxed{\mathcal{S}_{\mathcal{M}} = (\mathcal{C}, x_1, x_2).} \tag{4.7}$$

4.3. Symplectic Invariants of a Spectral Curve

Once we have found the spectral curve $\mathcal{S}_{\mathcal{M}}$ of our matrix model, we can compute the coefficients F_g in the topological expansion of its partition function,

$$\ln Z_{\mathcal{M}} = \sum_{g=0}^{\infty} g_s^{2g-2} F_g,$$

by computing the symplectic invariants of this curve,

$$F_g = F_g(\mathcal{S}_{\mathcal{M}}),$$

following [3].

Let us recall the definition of these invariants for an arbitrary spectral curve $\mathcal{S}$.

Let $\mathcal{S} = (\mathcal{C}, x, y)$ be a spectral curve, comprised of the data of a Riemann surface $\mathcal{C}$ and two functions $x(z), y(z) : \mathcal{C} \to \mathbb{C}$, meromorphic on $\mathcal{C}$ away from a finite set of points (we wish to allow logarithms). We will assume that $\mathrm{d}x$ is a meromorphic form on all of $\mathcal{C}$.

4.3.1. Branchpoints. Let a_i be the branch points of the function x,

$$\mathrm{d}x(a_i) = 0.$$

We assume that all branch points are simple,[5] i.e. that $\mathrm{d}x$ has a simple zero at a_i. This implies that in the vicinity of a_i, the map x is $2:1$. We introduce the notation $\bar{z} \neq z$ such that

$$x(\bar{z}) = x(z).$$

$\bar{z}$ is called the conjugate point to z, and it is defined only in the vicinity of branch points, as depicted in Fig. 6.

[5] There also exists a version of the topological recursion for branch points that are not simple [40]. However, we will not need this here: we will show that the spectral curve we find in Sect. 5 is symplectically equivalent to the mirror curve; for generic Kähler parameters, the latter has only simple branch points.

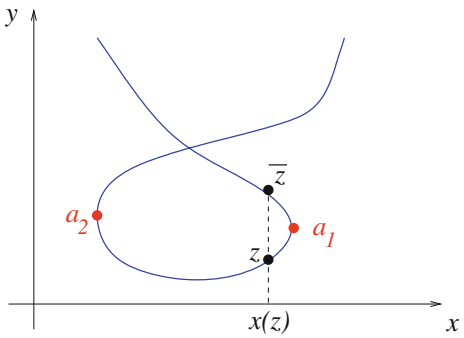

FIGURE 6. At a regular branch point $a \in \mathcal{C}$ of x, y as a function of x has a branchcut $y \sim y(a) + C\sqrt{x - x(a)}$. If z is a point on one branch near a, we call $\bar{z}$ the conjugate point on the other branch; it has the same x projection, $x(\bar{z}) = x(z)$. Notice that $\bar{z}$ is defined only locally near branch points. If we follow z from a_1 to a_2, $\bar{z}$ may have to jump from one branch to another

We also require that the branch points of x and y do not coincide, such that $\mathrm{d}y(a_i) \neq 0$ and $y(z)$ therefore has a square-root branchcut as a function of x at $x(a_i)$. If y is finite at a_i, its local behavior is hence given by

$$y(z) \sim y(a_i) + C_i\sqrt{x(z) - x(a_i)}.$$

If a_i corresponds to a hard edge, we require y to have a pole here. Its local behavior is hence given by

$$y(z) \sim \frac{C_i}{\sqrt{x(z) - x(a_i)}}.$$

4.3.2. Bergman Kernel. On a curve $\mathcal{C}$, there exists a unique symmetric 2-form $B(z_1, z_2)$ with a double pole on the diagonal $z_1 = z_2$ and no other poles, with the following normalization on $\mathcal{A}$-cycles,

$$\oint_{z_2 \in \mathcal{A}_{j,i}} B(z_1, z_2) = 0.$$

In any local coordinate near $z_1 = z_2$, one has

$$B(z_1, z_2) \sim \frac{\mathrm{d}z_1 \mathrm{d}z_2}{(z_1 - z_2)^2} + \text{regular}.$$

B is called the Bergman kernel of $\mathcal{C}$, or the fundamental 2-form of the second kind [41].

4.3.3. Recursion Kernel. We now define the recursion kernel K as

$$K(z_0, z) = \frac{\int_{\bar{z}}^{z} B(z_0, z')}{2(y(\bar{z}) - y(z))\mathrm{d}x(z)}.$$

This kernel is a globally defined 1-form in the variable $z_0 \in \mathcal{C}$. In the variable z, it is the inverse of a 1-form (that means we have to multiply it with a quadratic differential before computing any integral with it); it is defined only locally near branch points of x, such that $K(z_0, \bar{z}) = K(z_0, z)$. At the branch points, it has simple poles,

$$K(z_0, z) \sim -\frac{B(z_0, z)}{2\mathrm{d}x(z)\mathrm{d}y(z)} + \text{regular}.$$

4.3.4. Topological Recursion. Correlation forms $W_n^{(g)}(z_1, \ldots, z_n)$ (not to be confused with the resolvents $W_i(z)$ introduced above) are symmetric n-forms defined by

$$W_1^{(0)}(z) = -y(z)\mathrm{d}x(z),$$
$$W_2^{(0)}(z_1, z_2) = B(z_1, z_2),$$

and then by recursion (we write collectively $J = \{z_1, \ldots, z_n\}$),

$$W_{n+1}^{(g)}(z_0, J) = \sum_i \operatorname*{Res}_{z \to a_i} K(z_0, z) \left[W_{n+2}^{(g-1)}(z, \bar{z}, J) + \sum_{h=0}^{g} {\sum_{I \subset J}}' W_{1+|I|}^{(h)}(z, I) W_{1+n-|I|}^{(g-h)}(\bar{z}, J \setminus I) \right]$$

where $\sum_I'$ is the sum over all subsets of J, restricted to $(h, I) \neq (0, \emptyset)$ and $(h, I) \neq (g, J)$.

Although it is not obvious from the definition, the forms $W_n^{(g)}$ are symmetric. For $2 - 2g - n < 0$, they are meromorphic n-forms with poles only at branch points. These poles are of degree at most $6g - 4 + 2n$, and have vanishing residues.

For the one matrix model, the $W_n^{(g)}$ coincide with the n-point function of the trace of the resolvent at order g in the topological expansion.

4.3.5. Symplectic Invariants. Finally, for $g \geq 2$, we define the symplectic invariants F_g (also denoted $W_0(g)$ in [8]) by

$$F_g(\mathcal{S}) = \frac{1}{2 - 2g} \sum_i \operatorname*{Res}_{z \to a_i} \Phi(z) W_1^{(g)}(z),$$

where Φ is any function defined locally near branch points of x such that $d\Phi = y\mathrm{d}x$.

The definitions of F_1 and F_0 are more involved and we refer the reader to [8]. F_0 is called the prepotential, and F_1 is closely related to the determinant of the Laplacian on $\mathcal{C}$ with metrics $|ydx|^2$, see [42,43].

In [8], it was proved that if the spectral curve is algebraic then the $F_g(\mathcal{S})$'s depend only on the orbit of $\mathcal{S}$ under the group of transformations generated by

$\mathfrak{R}: \mathcal{S} \mapsto \tilde{\mathcal{S}} = (\mathcal{C}, x, y + R(x))$ where $R(x)$ is any rational function of x,

$\mathfrak{F}: \mathcal{S} \mapsto \tilde{\mathcal{S}} = (\mathcal{C}, f(x), y/f'(x))$ where $f(x)$ is an analytical function of x, with f' rational, such that $df = f'\mathrm{d}x$ has the same number of zeroes as $\mathrm{d}x$,

$\mathfrak{S}: \mathcal{S} \mapsto \tilde{\mathcal{S}} = (\mathcal{C}, y, -x)$.

These three transformations are symplectic, i.e. they leave $\mathrm{d}x \wedge \mathrm{d}y$ invariant, whence the name "symplectic invariants."

Remark. *For every spectral curve $\mathcal{S}$, not necessarily algebraic, $F_g(\mathcal{S})$ is always invariant under $\mathfrak{R}$ and $\mathfrak{F}$. This can be seen directly from the definitions, since the recursion kernel is itself invariant under $\mathfrak{R}$ and $\mathfrak{F}$.*

The invariance under $\mathfrak{S}$ was proved only for algebraic curves, and we do not know to what extent it holds for non-algebraic spectral curves. Luckily, we will not need to invoke the transformation $\mathfrak{S}$ in this paper.

The symplectic invariants are homogeneous of degree $2-2g$,

$$F_g(\mathcal{C}, x, \lambda y) = \lambda^{2-2g} F_g(\mathcal{C}, x, y). \tag{4.8}$$

In particular, they are invariant under the parity transformation $F_g(\mathcal{C}, x, -y) = F_g(\mathcal{C}, x, y)$.

5. The Spectral Curve for the Topological tring's Matrix Model

Applying the procedure outlined in Sect. 4.2.2 to our matrix model, we will determine a spectral curve $\mathcal{S}_{\mathcal{M}_{\mathfrak{X}_0}}$ in this section. [3] demonstrated that for a chain of matrices, we have

$$\ln Z_{\mathcal{M}} = \sum_g g_s^{2g-2} F_g(\mathcal{S}_{\mathcal{M}}),$$

with F_g the symplectic invariants of [8].

In our case, there is a subtlety here. The potentials of our matrix model depend explicitly on g_s. The spectral curve $\mathcal{S}_{\mathcal{M}}$ constructed by the rules of Sect. 4.2.2 above is hence going to depend on g_s as well. One might therefore reasonably expect that the $F_g(\mathcal{S}_{\mathcal{M}})$ also depend on g_s, and write a g_s expansion:

$$F_g(\mathcal{S}_{\mathcal{M}}) \stackrel{?}{=} \sum_k g_s^k F_{g,k}.$$

We shall argue in Sect. 5.3, however, that the spectral curve $\mathcal{S}_{\mathcal{M}}$ is symplectically equivalent to the mirror spectral curve $\mathcal{S}_{\hat{\mathfrak{X}}_0}$ of Sect. 2.2,

$$\mathcal{S}_{\mathcal{M}} \sim \mathcal{S}_{\hat{\mathfrak{X}}_0}.$$

The latter is independent of g_s. Since the F_g's are symplectic invariants, this will imply that the $F_g(\mathcal{S}_{\mathcal{M}})$ are in fact independent of g_s.

In our case, since we have engineered our matrix model to yield Gromov–Witten invariants $F_g^{\mathrm{top}}(\mathfrak{X}_0)$ as its partition function, re-computing the partition function via the methods of [3] will yield

$$F_g^{\mathrm{top}}(\mathfrak{X}_0) = F_g(\mathcal{S}_{\mathcal{M}}) = F_g(\mathcal{S}_{\hat{\mathfrak{X}}_0}).$$

This will imply the BKMP conjecture for $\mathfrak{X}_0$, i.e.

$$F_g^{\rm top}(\mathfrak{X}_0) = F_g(\mathcal{S}_{\hat{\mathfrak{X}}_0}).$$

5.1. Applying the Chain of Matrices Rules

We now apply the rules of Sect. 4.2.2 to the chain of matrices model introduced in Sect. 3.

- Following condition 1 of Sect. 4.2.2, we consider a Riemann surface $\mathcal{C}$ and functions $x_i(z), i = 0, \ldots, m+1$, associated to the matrices M_i, and functions $y_i(z), i = 1, \ldots, m+1$, associated to the matrices R_i, as well as two additional functions $y_0(z)$ and $y_{m+2}(z)$ at the ends of the chain. The conditions enumerated in Sect. 4.2.2 will allow us to specify $\mathcal{C}$ as well as the functions x_i and y_i:
  - Since there is no potential for the matrices R_i, Eq. (4.4) implies that we have, for $i = 1, \ldots, m+1$,
  $$x_i(z) - x_{i-1}(z) = 0.$$
  We can hence suppress the index i on these functions, $x(z) = x_i(z)$.
  - For $i = 1, \ldots, m$, Eq. (4.4) gives
  $$y_i(z) - y_{i+1}(z) = 2V'_{\vec{a}_i}(x(z)) - V'_{\vec{a}_{i+1}}(x(z)) - V'_{\vec{a}_{i-1}}(x(z)) - g_s \frac{f_i'(x(z))}{f_i(x(z))} - \frac{g_s S_i + i\pi}{x(z)}$$
  and
  $$y_0(z) - y_1(z) = V'_{\vec{a}_0}(x(z)) - V'_{\vec{a}_1}(x(z)) - g_s \frac{f_0'(x(z))}{f_0(x(z))},$$
  $$y_{m+1}(z) - y_{m+2}(z) = V'_{\vec{a}_{m+1}}(x(z)) - V'_{\vec{a}_m}(x(z)) - g_s \frac{f_{m+1}'(x(z))}{f_{m+1}(x(z))}.$$
  More explicitly, in terms of the quantum digamma-function
  $$\psi_q(x) = xg'(x)/g(x),$$
  whose small g_s expansion is given by a Stirling-like formula:
  $$\psi_q(x) = -\frac{1}{\ln q} \sum_{n=0}^{\infty} \frac{(-1)^n B_n}{n!} (\ln q)^n \mathrm{Li}_{1-n}(1/\mathrm{x})$$
  $$= \frac{1}{\ln q} \left[\ln\left(1 - \frac{1}{x}\right) - \frac{\ln q}{2(x-1)} - \sum_{n=1}^{\infty} \frac{B_{2n}}{(2n)!} (\ln q)^{2n} \mathrm{Li}_{1-2n}(\mathrm{x}) \right],$$
  (see appendix A of [1]), we obtain
  $$\begin{aligned} x(z)(y_{i+1}(z) - y_i(z)) &= i\pi + g_s S_i - g_s \sum_j (2\psi_q(q^{a_{j,i}}/x(z)) - \psi_q(q^{a_{j,i+1}}/x(z)) \\ &\quad - \psi_q(q^{a_{j,i-1}}/x(z))) \\ &\quad + g_s \frac{x(z) f_i'(x(z))}{f_i(x(z))}, \end{aligned} \tag{5.1}$$

as well as

$$x(z)(y_1(z)-y_0(z)) = -g_s\sum_j \psi_q(q^{a_{j,0}}/x(z)) + g_s\sum_j \psi_q(q^{a_{j,1}}/x(z)) \\ -g_s\sum_j\sum_{k=0}^{d-1}\frac{x(z)}{x(z)-q^{a_{j,0}+k}},$$

$$x(z)(y_{m+2}(z)-y_{m+1}(z)) = -g_s\sum_j \psi_q(q^{a_{j,m+1}}/x(z)) + g_s\sum_j \psi_q(q^{a_{j,m}}/x(z)) \\ -g_s\sum_j\sum_{k=0}^{d-1}\frac{x(z)}{x(z)-q^{a_{j,m+1}+k}}$$

Note that we have explicitly used the fact that the partitions $\alpha_{j,m+1}$ and $\alpha_{j,0}$ are chosen to be trivial, i.e. we have chosen

$$f_0'(x)/f_0(x) = \sum_j\sum_{k=0}^{d-1} 1/(x-q^{a_{j,0}+k}),$$

$$f_{m+1}'(x)/f_{m+1}(x) = \sum_j\sum_{k=0}^{d-1} 1/(x-q^{a_{j,m+1}+k}).$$

– Since the integral over R_i is over $H_N(\mathbb{R}_+)$, i.e. its eigenvalues are integrated on $\mathbb{R}_+$, the integration contour has an endpoint (hard edge) at $y_i = 0$. Condition 2 hence requires that at a pre-image $y_i^{-1}(0)$, which we will refer to as ∞_i, the following holds

$$y_i(\infty_i) = 0, \quad \mathrm{d}y_i(\infty_i) = 0, \quad x(z) \text{ has a simple pole at } z = \infty_i.$$

Furthermore, introducing a local parameter z in the neighborhood of ∞_i, the above translates into

$$y_i(z) \sim \mathcal{O}(z^2), \quad x(z) \sim 1/z.$$

Hence, $\forall i = 1, \dots, m+1$,

$$y_i \sim_{\infty_i} \mathcal{O}(1/x^2).$$

- This behavior together with the relations (5.1) imply that near ∞_i, we have

$$x(y_{j+1}-y_j) \underset{z\to\infty_i}{\sim} i\pi + g_s S_j + g_s\sum_{l=0}^{n}(2a_{l,j}-a_{l,j+1}-a_{l,j-1}) + O(1/x).$$

In particular, it follows that y_j near ∞_i behaves in $1/x$ and not as $O(1/x^2)$ and thus $\infty_j \neq \infty_i$. Thus, all points $\{\infty_1, \dots, \infty_{m+1}\} \subset x^{-1}(\infty)$ are distinct , i.e. condition 2 requires that $x^{-1}(\infty)$ have at least $m+1$ points.

Since there is no potentials for matrices R_i's, Condition 3 implies that $x(z)$ can have no other singularities, and therefore $x^{-1}(\infty)$ has exactly $m+1$ elements that are simple poles of x. This implies that the function $x : z \mapsto x(z)$ is a meromorphic function on $\mathcal{C}$ of degree $m+1$. In particular, any point $x \in \mathbb{C}$ has $m+1$ preimages in $\mathcal{C}$.

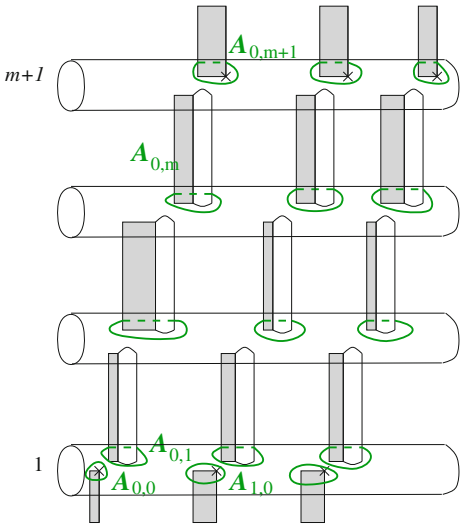

FIGURE 7. The spectral curve of our matrix model can be represented as follows. The cover of $\mathbb{CP}^1$ provided by x has $m+1$ sheets. Instead of the projective plane of x, we represent the sheets of $\ln x$, which are cylinders. Cycles $\mathcal{A}_{j,i}$ appear in sheets $i-1$ and i. They enclose singularities of the resolvent W_i. Algebraic cuts are represented as *vertical cylinders*, and poles and log singularities are represented as *grey strips*. There is only one cycle $\mathcal{A}_{j,0}$ (which is in sheet 0) and one $\mathcal{A}_{j,m+1}$ (in sheet m), and they enclose only poles or log singularities of y_0, respectively y_{m+1}

- We thus see that the Riemann surface $\mathcal{C}$ can be realized as an $m+1$ sheeted covering of the x-plane $\mathbb{P}^1$.
- By condition 5, since for $i = 0, \ldots, m+2$ there are d eigenvalues of M_i of the form $q^{a_{j,i}+\mathbb{N}}$ surrounded by the path $\widehat{\mathcal{A}}_{j,i}$, we have the $(m+2)\times(n+1)$ filling fraction conditions

$$\frac{1}{2i\pi}\oint_{\mathcal{A}_{j,i}} y_i \mathrm{d}x = dg_s \qquad \text{for } i = 0, \ldots, m+1, \quad j = 0, \ldots, n.$$

x defines an $m+1$ sheeted cover of $\mathbb{CP}^1$ with sheets defined in accord with Condition 4. Considering the function $\ln x$ instead, with singularities at $x = 0$ and $x = \infty$, each sheet of this cover is mapped to a cylinder. We have depicted this covering in Fig. 7, and indicated the singularities of y_i on each sheet: algebraic cuts are represented by vertical cylinders, and poles and logarithmic cuts by grey strips.

In sheet i we have represented some contours $\mathcal{A}_{j,i}$ whose image under the projection $x : \mathcal{C} \to \mathbb{CP}^1$ surround all points of type $q^{a_{j,i}+\mathbb{N}}$.

For $i = 1, \ldots, m$, the resolvent $W_i(x)$ of the ith matrix M_i is computed as a contour integral around the sum over j of cycles $\mathcal{A}_{j,i}$ on sheet i,

$$W_i(x) = \sum_{j=0}^{n} \frac{1}{2i\pi} \oint_{\mathcal{A}_{j,i}} \frac{y_i(z')\mathrm{d}x(z')}{x - x(z')}.$$

In addition, as argued in [1], the potentials of M_0 and M_{m+1} are such that in fact the matrices M_0 and M_{m+1} are frozen, and thus their resolvents contain only poles. In terms of the functions y_0 and y_{m+1}, we conclude that the singularities of y_0 in $\mathcal{A}_{j,0}$ in sheet 1 and the singularities of y_{m+1} in $\mathcal{A}_{j,m+1}$ in sheet $m+1$ can be only poles, not cuts.

5.2. Symplectic Change of Functions

The spectral curve of the matrix model is $\mathcal{S}_{\mathrm{MM}} = (\mathcal{C}, x, y_0)$, and our goal is to relate it to the mirror curve described in Sect. 2.2. The mirror curve is described via the algebraic equation (2.5) in the two functions $x_1, x_2 : \mathcal{C}_{\mathrm{mirror}} \to \mathbb{CP}^1$ (in the patch $x_0 = 1$). We wish to obtain a similar algebraic description of $\mathcal{C}$. Due to log singularities in y_0, to be traced to the small g_s behavior of $\psi_q(x)$, an algebraic equation in the variables (x, y_0) cannot exist (recall that x is meromorphic). In this section, we shall, via a series of symplectic transformations on the y_i of the type enumerated in Sect. 4.3.5, arrive at functions Y_i that are meromorphic on $\mathcal{C}$, and hence each present a viable candidate to pair with x to yield an algebraic equation for $\mathcal{C}$.

Essentially, we wish to introduce the exponentials of y_i. While this will eliminate the log singularities, poles in y_i would be elevated to essential singularities. We hence first turn to the question of eliminating these poles.

5.2.1. The Arctic Circle Property. On the physical sheet, the interpretation of a pole of y_i is as an eigenvalue of the matrix M_i with delta function support. Such a so-called frozen eigenvalue can arise in the following way.

The sum over all partitions is dominated by partitions close to a typical equilibrium partition, i.e. a saddle point. The typical partition has a certain typical length referred to as its equilibrium length $\bar{n}$. All partitions with a length very different from the equilibrium length contribute only in an exponentially small way (and thus non-perturbatively) to the full partition function. Introducing a cutoff on the length of partitions which is larger than the equilibrium length hence does not change the perturbative part of the partition function. Now recall that when we defined the $h_i(\gamma)$ of a representation γ in Appendix A, we introduced an arbitrary maximal length d such that $l(\gamma) \leq d$ and set

$$h_i(\gamma) = a_\gamma + d - i + \gamma_i.$$

Setting $\gamma_i = 0$ for $d \geq i > \bar{n}$ yields h_i that do not depend on the integration variables, hence are frozen at fixed values. This behavior is referred to as the

arctic circle property [44], as all eigenvalues beyond the arctic circle situated at equilibrium length $\bar{n}$ are frozen.

Returning to our matrix model, the eigenvalues of the matrices M_i are given by $q^{(h_{j,i})_l}$. For $d \geq l > n_{j,i}$, they are frozen, and thus contribute poles to y_i by (4.5) (recall that poles of the resolvent correspond to eigenvalues with delta function support) in the physical sheet. We will assume that these are the only poles in the physical sheet (this is one of the "minimality assumptions" that we make and refer to in Sect. 5.5 and in our concluding Sect. 7) and we subtract them to obtain new functions $\tilde{y}_i$,

$$\tilde{y}_0(z) = x(z)y_0(z) - \sum_j \sum_{k=0}^{d-1} \frac{g_s x(z)}{x(z) - q^{a_{j,0}+k}},$$
$$\tilde{y}_{m+2}(z) = x(z)y_{m+2}(z) + \sum_j \sum_{0}^{d-1} \frac{g_s x(z)}{x(z) - q^{a_{j,m+1}+k}}$$

and for $i = 1, \ldots, m+1$,

$$\tilde{y}_i(z) = x(z)y_i(z) - \sum_j \sum_{k=0}^{d-n_{j,i}-1} \frac{g_s x(z)}{x(z) - q^{a_{j,i}+k}} + \sum_j \sum_{k=0}^{d-n_{j,i-1}-1} \frac{g_s x(z)}{x(z) - q^{a_{j,i-1}+k}}.$$

We have set

$$n_{j,0} = 0, \quad n_{j,m+1} = 0.$$

Notice that at large $x(z)$ in sheet i we have

$$\tilde{y}_0 \sim O(1/x(z)), \qquad \tilde{y}_{m+2} \sim O(1/x(z))$$

and for $i = 1, \ldots, m+1$

$$\tilde{y}_i \sim g_s \sum_j (n_{j,i} - n_{j,i-1}) + O(1/x(z)).$$

As a general property of ψ_q, we have for any integer $n_{j,i} \leq d$

$$\psi_q(q^{a_{j,i}}/x) = \psi_q(q^{a_{j,i}+d-n_{j,i}}/x) + \sum_{k=0}^{d-n_{j,i}-1} \frac{x}{x - q^{a_{j,i}+k}}.$$

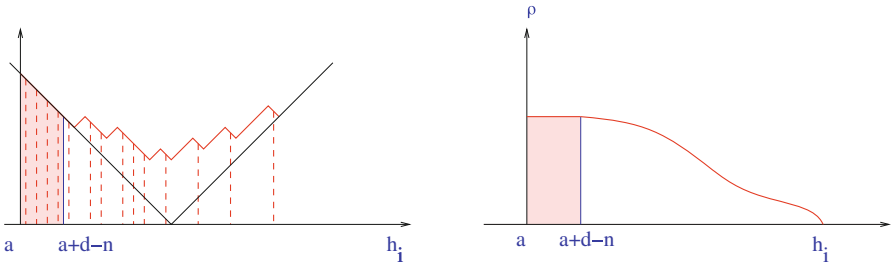

FIGURE 8. We shift the cut-off d on the representation lengths, $d \to n_{j,i}$, with $n_{j,i}$ chosen such that frozen eigenvalues in the expected distribution of the h_i are suppressed. In the limit of vanishing spacing ($g_s \to 0$), the equidistant frozen eigenvalues give rise to a constant eigenvalue density region

Hence, the loop equations for the new functions $\tilde{y}_i$ read

$$\begin{aligned}
&\tilde{y}_{i+1}(z) - \tilde{y}_i(z) \\
&\quad = i\pi + g_s S_i + g_s \sum_j (2\psi_q(q^{a_{j,i}+d-n_{j,i}}/x(z)) - \psi_q(q^{a_{j,i+1}+d-n_{j,i+1}}/x(z)) \\
&\qquad - \psi_q(q^{a_{j,i-1}+d-n_{j,i-1}}/x(z))) + g_s \frac{x(z) f_i'(x(z))}{f_i(x(z))}, \\
&\tilde{y}_1(z) - \tilde{y}_0(z) \\
&\quad = g_s \sum_j \psi_q(q^{a_{j,0}+d}/x(z)) - g_s \sum_j \psi_q(q^{a_{j,1}+d-n_{j,1}}/x(z)), \\
&\tilde{y}_{m+2}(z) - \tilde{y}_{m+1}(z) \\
&\quad = g_s \sum_j \psi_q(q^{a_{j,m+1}+d}/x(z)) - g_s \sum_j \psi_q(q^{a_{j,m}+d-n_{j,m}}/x(z)).
\end{aligned}$$

The $n_{j,i}$ in the above definitions are defined as the equilibrium lengths, i.e. by the property that the functions $\tilde{y}_i$ have no poles on their physical sheet. That such a choice of $n_{j,i}$ exists is suggested by the arctic circle property (Fig. 8).

Note that the $n_{j,i}$ can also be specified by the fact that $q^{a_{j,i}+d-n_{j,i}}$ be the beginning of the cut encircled by $\gamma_{j,i}$. As we have identified the discontinuities of y_i to lie across branchcuts of x, this implies that x has ramification points at the element of $x^{-1}(q^{a_{j,i}+d-n_{j,i}})$ lying on the physical sheets of y_i.

Note that the arctic circle property also implies the perturbative independence of our expressions from the arbitrary cut-off d. Changing d to $d + d'$ merely introduces d' new frozen eigenvalues h_i. This independence from d is important in establishing the equality between the topological string partition function and our matrix integral (3.1), as the topological vertex formulae in fact are formulated in the limit $d \to \infty$.

5.2.2. Obtaining Globally Meromorphic Functions. We have arrived at functions $\tilde{y_i}$ that have no poles on their physical sheet, and are thus safely exponentiated there. We wish now to use the loop equations to obtain functions which are globally well-behaved.

To this end, we note that since the Gromov–Witten invariants are defined as a formal power series in g_s, we can compute the spectral curve order by order in g_s, invoking the following small $\ln q$ expansion [1]:

$$\psi_q\left(q^{a_{j,i}+d-n_{j,i}}/x\right) \sim -\frac{1}{g_s}\ln\left(1-\frac{x}{q^{a_{j,i}+d-n_{j,i}}}\right)+\frac{x}{2(x-q^{a_{j,i}+d-n_{j,i}})} + \frac{1}{g_s}\sum_{n=1}^{\infty}\frac{B_{2n}g_s^{2n}}{(2n)!}\mathrm{Li}_{1-2n}\left(\mathrm{q}^{\mathrm{d}-\mathrm{n_{j,i}}+\mathrm{a_{j,i}}}/\mathrm{x}\right).$$

The functions f_i'/f_i are completely non-perturbative; one can easily check with the above expansion that they can be replaced by 0 to every order in g_s.

Introducing new functions $X(z)$ and Y_i by the formulae

$$\begin{aligned} x(z) &= q^d X(z), \\ \tilde{y}_0(z) &= \ln Y_0(z), \\ \tilde{y}_{m+2}(z) &= \ln Y_{m+2}(z), \end{aligned}$$

and for $i = 1, \ldots, m+1$

$$\begin{aligned} \tilde{y}_i(z) = \ln Y_i(z) &+ \sum_j \frac{X(z)g_s}{2(X(z)-q^{a_{j,i}-n_{j,i}})} \\ &+\frac{1}{g_s}\sum_j\sum_{n=1}^{\infty}\frac{B_{2n}g_s^{2n}}{(2n)!}\mathrm{Li}_{1-2n}(\mathrm{q}^{\mathrm{a_{j,i}}-\mathrm{n_{j,i}}}/\mathrm{X(z)}) \\ &-\sum_j \frac{X(z)g_s}{2(X(z)-q^{a_{j,i-1}-n_{j,i-1}})} \\ &-\frac{1}{g_s}\sum_j\sum_{n=1}^{\infty}\frac{B_{2n}g_s^{2n}}{(2n)!}\mathrm{Li}_{1-2n}(\mathrm{q}^{\mathrm{a_{j,i-1}}-\mathrm{n_{j,i-1}}}/\mathrm{X(z)}) \end{aligned}$$

yields loop equations that are algebraic on their right hand side,

$$\begin{aligned} \frac{Y_i}{Y_{i+1}} &= -e^{-g_s S_i}\prod_j \frac{(X-q^{a_{j,i+1}-n_{j,i+1}})(X-q^{a_{j,i-1}-n_{j,i-1}})}{(X-q^{a_{j,i}-n_{j,i}})^2} \\ &\quad\times\prod_j q^{2(a_{j,i}-n_{j,i})-(a_{j,i+1}-n_{j,i+1})-(a_{j,i-1}-n_{j,i-1})}, \\ \frac{Y_0}{Y_1} &= \prod_j \frac{(X-q^{a_{j,1}-n_{j,1}})}{(X-q^{a_{j,0}})}\prod_j q^{a_{j,0}-(a_{j,1}-n_{j,1})}, \\ \frac{Y_{m+1}}{Y_{m+2}} &= \prod_j \frac{(X-q^{a_{j,m}-n_{j,m}})}{(X-q^{a_{j,m+1}})}\prod_j q^{a_{j,m+1}-(a_{j,m}-n_{j,m})}, \end{aligned} \tag{5.2}$$

i.e.

$$\frac{Y_i}{Y_0} = e^{g_s(S_1+\cdots+S_{i-1})} \prod_j q^{(a_{j,i}-n_{j,i})-(a_{j,i-1}-n_{j,i-1})} \prod_j \frac{X - q^{a_{j,i-1}-n_{j,i-1}}}{X - q^{a_{j,i}-n_{j,i}}}.$$

Since we have argued that the Y_i are holomorphic on their physical sheet, and the ratio Y_i/Y_{i+1} is purely algebraic, we conclude that the Y_i are meromorphic functions on all of $\mathcal{C}$. This was the goal we had set out to achieve.

Note that the above changes of variables have modified the asymptotics at infinity and the integrals over the $\mathcal{A}$-cycles. More precisely, we have

$$\begin{aligned}
&\forall i \in [1, m+1] : \ln Y_i \underset{\infty_i}{\sim} \tilde{y}_i \underset{\infty_i}{\sim} g_s \sum_j (n_{j,i} - n_{j,i-1}) + O\left(\frac{1}{x}\right), \qquad (5.3)\\
&\ln Y_0 = \tilde{y}_0 \underset{\infty}{\sim} O\left(\frac{1}{x}\right),\\
&\ln Y_{m+2} = \tilde{y}_{m+2} \underset{\infty}{\sim} O\left(\frac{1}{x}\right).
\end{aligned}$$

The filling fraction equation reads

$$\frac{1}{2i\pi} \int_{\mathcal{A}_{j,i}} \frac{\tilde{y}_i(z)}{x(z)} \mathrm{d}x(z) = g_s(d - (d - n_{j,i})) = g_s n_{j,i}. \qquad (5.4)$$

In terms of Y_0, these conditions can be rewritten as

$$\ln Y_0 \underset{\infty_i}{\sim} -g_s(S_1 + \cdots + S_{i-1}) + g_s \sum_{j=0}^{n} (a_{j,i} - a_{j,i-1}) + O\left(\frac{1}{x}\right)$$

and

$$\begin{aligned}
\frac{1}{2i\pi} \int_{\mathcal{A}_{j,i}} \ln Y_0 \frac{\mathrm{d}X}{X} &= \frac{1}{2i\pi} \int_{\mathcal{A}_{j,i}} \ln Y_i \frac{\mathrm{d}X}{X} + \frac{1}{2i\pi} \int_{\mathcal{A}_{j,i}} \ln X d \ln\left(\frac{Y_i}{Y_0}\right)\\
&= \frac{1}{2i\pi} \int_{\mathcal{A}_{j,i}} \ln Y_i \frac{\mathrm{d}X}{X} + \frac{1}{2i\pi} \int_{\mathcal{A}_{j,i}} \ln X d\left(\sum_{k=1}^{i} \ln \frac{Y_k}{Y_{k-1}}\right)\\
&= \frac{1}{2i\pi} \int_{\mathcal{A}_{j,i}} \ln Y_i \frac{\mathrm{d}X}{X} - \frac{1}{2i\pi} \int_{\mathcal{A}_{j,i}} \ln X\\
&\quad \times \left(\sum_l \frac{\mathrm{d}X}{X - q^{a_{l,i}-n_{l,i}}} - \frac{\mathrm{d}X}{X - q^{a_{l,i-1}-n_{l,i-1}}}\right)\\
&= \frac{1}{2i\pi} \int_{\mathcal{A}_{j,i}} \ln Y_i \frac{\mathrm{d}X}{X} + g_s(a_{j,i} - n_{j,i})\\
&= g_s n_{j,i} + g_s(a_{j,i} - n_{j,i})\\
&= g_s a_{j,i}.
\end{aligned}$$

5.3. Recovering the Mirror Curve

We have argued above that X and Y_i, and hence in particular Y_0, are meromorphic functions on $\mathcal{C}$. There must hence exist a polynomial $H(X,Y)$ such that (see e.g. Theorem 5.8.1 in [45])

$$H(X,Y_0)=0.$$

The facts that X provides an $m+1$ sheeted cover of $\mathbb{CP}^1$ and that Y_0 may have $n+1$ poles in its physical sheet imply that the polynomial H has degrees at least $(n+1,m+1)$. As announced in the introduction, we shall choose the minimal hypothesis that it has exactly these degrees. Thus,

$$H(X,Y)=\sum_{i=0}^{m+1}\sum_{j=0}^{n+1}H_{i,j}X^jY^i. \tag{5.5}$$

As we saw in Sect. 2.2, projectivizing a generic polynomial of these degrees (yielding a homogeneous polynomial of degree $m+n+2$) indeed gives rise to a curve of genus $\mathfrak{g}=nm$.

We now need to determine the $(n+2)(m+2)-1$ unknown coefficients of H (H is defined up to a global multiplicative constant).

The cycle integrals

$$\oint_{\mathcal{A}_{j,i}}\ln Y_0\frac{\mathrm{d}X}{X}=2i\pi g_s a_{j,i}$$

provide $(n+1)m$ constraints on the coefficients of H. We also have $m+1$ constraints for the behavior at $\infty_i, i=1,\dots,m+1$,

$$\operatorname*{Res}_{\infty_i}\ln Y_0\frac{\mathrm{d}X}{X}=g_s(S_1+\cdots+S_{i-1})-g_s\sum_{j=0}^{n}(a_{j,i}-a_{j,i-1}).$$

Finally, requiring that Y_0 has poles at $q^{a_{j,0}}$ and Y_{m+2} has zeroes at $q^{a_{j,m+1}}$ gives another $2(n+1)$ constraints, which we may write as

$$\operatorname*{Res}_{q^{a_{j,0}}}\ln X\frac{dY_0}{Y_0}=g_s a_{j,0},$$

$$\operatorname*{Res}_{q^{a_{j,m+1}}}\ln X\frac{dY_{m+2}}{Y_{m+2}}=g_s a_{j,m+1}.$$

This gives enough equations to completely determine H. Knowing H, we know the location of branch points as functions of $a_{j,i}$'s and S_i's, and can hence determine the $n_{j,i}$ by requiring that $q^{a_{j,i}-n_{j,i}}$ be a branch point.

Notice that we can choose to express the period integrals in any linear combination of $\mathcal{A}$-cycles. In particular,

$$\oint_{\mathcal{A}_{j,i+1}-\mathcal{A}_{j,i}}\ln Y_0\frac{\mathrm{d}X}{X}=2i\pi g_s(a_{j,i+1}-a_{j,i})=2i\pi t_{j,i},$$

$$\oint_{\mathcal{A}_{j,i+1}-\mathcal{A}_{j+1,i}}\ln Y_0\frac{\mathrm{d}X}{X}=2i\pi g_s(a_{j,i+1}-a_{j+1,i})=2i\pi r_{j,i}.$$

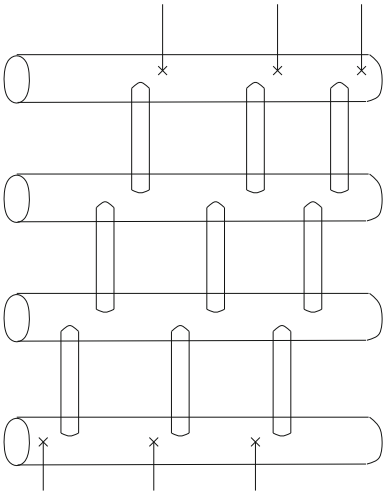

FIGURE 9. The spectral curve $(X, \frac{1}{X}\ln(Y_0))$ has the following structure: $X(z)$ is a meromorphic function of degree $m+1$ on a curve of genus $\mathfrak{g} = nm$. Therefore, it has $m+1$ poles and $m+1$ zeroes. It provides a branched covering of $\mathbb{CP}^1$. We prefer to represent $\ln X$ instead of X, and thus we have $m+1$ copies of the $\ln X$-cylinder. In each sheet there is one zero and one pole of X. Y_0 is a meromorphic function of degree $n+1$, so that it has $n+1$ zeroes in sheet 0, and $n+1$ poles in sheet $m+1$. We recognize the mirror curve $\mathcal{S}_{\hat{\mathfrak{X}}_0}$, which is a thickening of the toric web diagram

Similarly, we may also take linear combinations of $\mathcal{A}$-cycles together with circles surrounding the poles or zeroes of x in order to get the $s_{j,i}$ classes. We hence conclude that the periods of the curve $H(X, Y_0) = 0$ yield the quantum corrected Kähler parameters of the fiducial toric geometry $\mathfrak{X}_0$, allowing us to identify it with the corresponding mirror curve (Fig. 9).

5.4. Topological Expansion and Symplectic Invariants

Following [3], we obtained

$$\mathcal{S}_{\mathcal{M}} = (\mathcal{C}, x, y_0)$$

as the spectral curve of our matrix model at the end of Sect. 5.1.

As reviewed in Sect. 4.3, we can compute the corresponding symplectic invariants $F_g(\mathcal{S}_{\mathcal{M}})$, which assemble to yield the matrix model partition function [3],

$$\ln Z_{\mathcal{M}} = \sum_g g_s^{2g-2} F_g(\mathcal{S}_{\mathcal{M}}).$$

The symplectic transformation $\mathfrak{R}$ of Sect. 4.3.5 maps $(\mathcal{C}, x, y_0)$ to $(\mathcal{C}, x, \frac{1}{x}\ln Y_0)$ order by order in g_s. $\mathfrak{F}$ maps this to $(\mathcal{C}, X, \frac{1}{X}\ln Y_0)$, and a second application

of $\mathfrak{F}$ yields

$$\hat{\mathcal{S}}_{\mathcal{M}} = (\mathcal{C}, \ln X, \ln Y_0).$$

By the symplectic invariance of the F_g, we therefore have, order by order in powers of g_s,

$$F_g(\mathcal{S}_{\mathcal{M}}) = F_g(\hat{\mathcal{S}}_{\mathcal{M}}).$$

Since our matrix model was engineered to reproduce the Gromov–Witten invariants of $\mathfrak{X}_0$, we have arrived at

$$F_g^{\text{top}}(\mathfrak{X}_0) = F_g(\mathcal{C}, \ln X, \ln Y_0),$$

with X and Y_0 obeying the algebraic equation

$$H_0(X, Y_0) = 0.$$

This coincides with the equation (2.5) describing the mirror curve of $\mathfrak{X}_0$.

Given our minimality assumptions on the spectral curve, we have thus derived the BKMP conjecture for the fiducial geometry $\mathfrak{X}_0$.

5.5. The Small q Limit and the Thickening Prescription

The above derivation of the spectral curve for the matrix model is not fully rigorous, as we have relied on making minimal assumptions along the way. Although the spectral curve we have found here satisfies all the constraints of Sect. 4.2.2, to prove that it is the spectral curve of our matrix model requires a uniqueness result which we currently do not have.

In this section, we provide a heuristic argument that the qualitative behavior of the spectral curve and the mirror curve coincide in the large radius regime. Note that in our matrix model, the A-model Kähler parameters are $g_s a_{i,j}$ and $g_s S_i$. Hence, the small q regime $q \to 0$, i.e. $g_s \to +\infty$, coincides with the large Kähler parameter regime.

From the topological vertex formalism point of view, the sum over intermediate partitions $\alpha_{j,i}$ is weighted by $q^{a_{j,i}|\alpha_{j,i}|}$, thus at small q only very small partitions contribute to the matrix integral. The eigenvalues of matrix M_i are $\{q^{\alpha_{j,i_l}+a_{j,i}+d-l}\}, j = 0, \ldots, n, l = 1, \ldots, d$, where α_{j,i_l} is the length of the lth row of the partition $\alpha_{j,i}$, so in this limit almost all $\alpha_{j,i_l} = 0$ i.e. almost all eigenvalues of M_i are frozen to the values $q^{a_{j,i}+d-l}$. By the arguments in Sect. 5.2.1, the resolvent $W_i(x)$ of our spectral curve hence behaves at small q as

$$W_i(x) \sim \sum_{j=0}^{n} \sum_{l=1}^{d} \frac{1}{x - q^{a_{j,i}-l+d}} + \text{ small cut near } q^{a_{j,i}+d}.$$

Pictorially, the size of the cuts is shrinking in this limit, replacing the spectral curve by its skeleton, i.e. the toric graph of our fiducial geometry, see Fig. 10.

As we pointed out above, the small q limit corresponds to the large curve class limit. In this limit, the distance between the vertices of the pairs of pants out of which the mirror curve is constructed is taken to infinity. Just as the spectral curve, the mirror curve thus collapses to its skeleton in the $q \to 0$ limit.

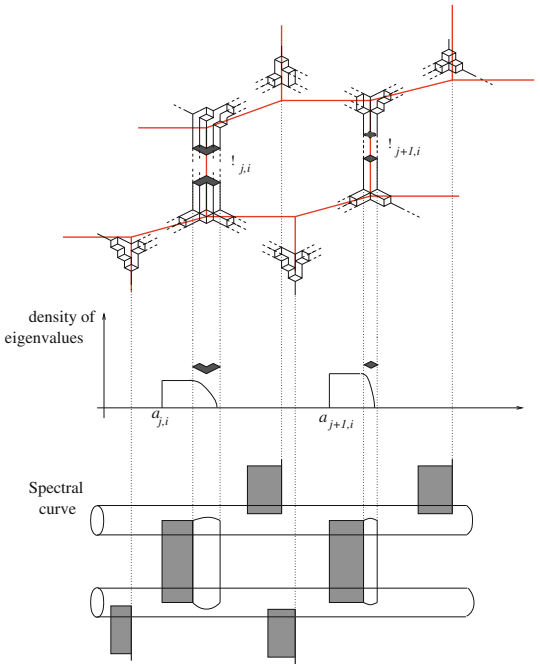

FIGURE 10. In the small q limit, only very small partitions contribute to the matrix integral, therefore the density of eigenvalues of M_i tends to the flat density (a Dirac comb of equidistant delta functions), the non-flat part, which reflects the cuts of the spectral cut, shrinks to zero

6. The General BKMP Conjecture

So far, we have obtained the BKMP conjecture only for the fiducial geometry $\mathfrak{X}_0$. Studying the behavior of the partition function under flop transitions will allow us to extend our argument to arbitrary toric geometries.

Every toric Calabi–Yau threefold can be obtained from a fiducial geometry, by a sequence of flops and then sending some Kähler parameters to ∞. As an example, in Fig. 13 we illustrate how to obtain the local $\mathbb{P}^2$ geometry from a 2×2 fiducial geometry.

6.1. Flop Invariance of Toric Gromov–Witten Invariants

Under the proper identification of curve classes, Gromov–Witten invariants (at least on toric manifolds) are invariant under flops. Assume the toric Calabi–Yau manifolds $\mathfrak{X}$ and $\mathfrak{X}^+$ are related via a flop transition, $\phi : \mathfrak{X} \to \mathfrak{X}^+$. In a neighborhood of the flopped $(-1,-1)$ curve, the respective toric diagrams are depicted in Fig. 11.

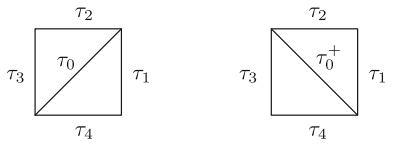

FIGURE 11. $\mathfrak{X}$ and $\mathfrak{X}^+$ in the vicinity of the $(-1,-1)$ curve

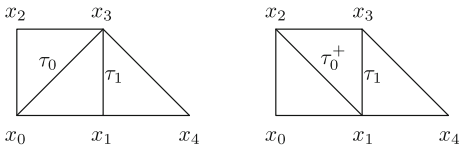

FIGURE 12. $\mathfrak{X}$ and $\mathfrak{X}^+$ in the vicinity of the $(-1,-1)$ curve

The 1-cones of $\Sigma_{\mathfrak{X}}$, corresponding to the toric invariant divisors of $\mathfrak{X}$, are not affected by the flop, hence can be canonically identified with those of $\mathfrak{X}^+$. The 2-cones τ_i in these diagrams correspond to toric invariant 2-cycles C_i, C_i^+ in the geometry. The curve classes of $\mathfrak{X}$ push forward to classes in $\mathfrak{X}^+$ via

$$\phi_*([C_0]) = -[C_0^+], \quad \phi_*([C_i]) = [C_i^+] + [C_0^+]. \tag{6.1}$$

All other curve classes $\vec{C}$ of $\mathfrak{X}$ are mapped to their canonical counterparts in $\mathfrak{X}^+$. Under appropriate analytic continuation and up to a phase factor (hence the $\propto$ in the following formula), the following identity then holds [32,46,47],

$$Z_{\mathrm{GW}}(\mathfrak{X}, Q_0, Q_1, \ldots, Q_4, \vec{Q}) \propto Z_{\mathrm{GW}}(\mathfrak{X}^+, 1/Q_0, Q_0Q_1, \ldots, Q_0Q_4, \vec{Q}), \tag{6.2}$$

i.e.

$$\mathrm{GW}_g(\mathfrak{X}, Q_0, Q_1, \ldots, Q_4, \vec{Q}) = \mathrm{GW}_g(\mathfrak{X}^+, 1/Q_0, Q_0Q_1, \ldots, Q_0Q_4, \vec{Q}). \tag{6.3}$$

6.2. Proof of Flop Invariance via Mirror Symmetry

Flop invariance of Gromov–Witten invariants upon the identification (6.1) is immediate upon invoking mirror symmetry, as (6.1) maps the mirror curve of $\mathfrak{X}$ to that of $\mathfrak{X}^+$. The proof is a simple computation (Fig. 12).

Let us introduce the notation t_0, t_1, t_0^+, t_1^+ for the Kähler volume of the curve classes C_i, C_i^+ corresponding to the respective 2-cones. In terms of these, we obtain for the mirror curve of $\mathfrak{X}$

$$x_0 + x_1 + x_2 + \frac{x_1x_2}{x_0}e^{T_0} + \frac{x_1^2}{x_0}e^{-T_1} = 0,$$

while the mirror curve of $\mathfrak{X}^+$ is given by

$$x_0 + x_1 + x_2 + \frac{x_1x_2}{x_0}e^{-T_0^+} + \frac{x_1x_3}{x_2}e^{-T_1^+} = 0.$$

Upon invoking $x_3 = \frac{x_1x_2}{x_0}e^{-T_0^+}$, we easily verify that the identification (6.1) maps these curves and their associated meromorphic 1-forms λ into each other.

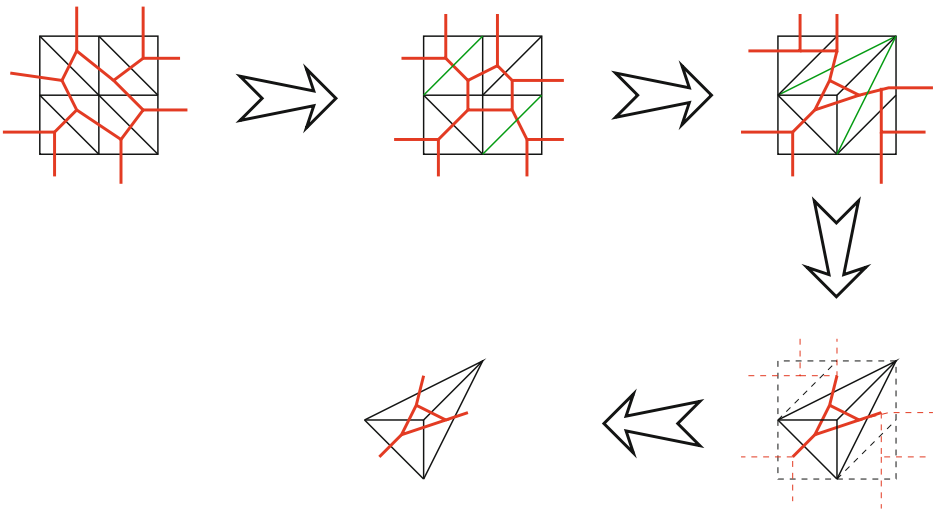

FIGURE 13. Example: We obtain local $\mathbb{P}^2$ from the fiducial geometry with 2×2 boxes by performing five flops and then sending the Kähler parameters of the unwanted compact edges to ∞

6.3. The BKMP Conjecture

Any toric Calabi–Yau manifold $\mathfrak{X}$ with Kähler moduli $\vec{Q}$ can be obtained from a sufficiently large fiducial geometry $(\mathfrak{X}_0, \vec{Q}_0)$ upon performing a series of flop transitions and taking unwanted Kähler moduli of $\mathfrak{X}_0$ to ∞, see Appendix B and see Fig. 13 for an example.

The Kähler moduli of $\mathfrak{X}$ are related to those of $\mathfrak{X}_0$ by some relation $\vec{Q} = f(\vec{Q}_0)$. We have just argued that the mirror curves of $\mathfrak{X}_0$ and $\mathfrak{X}$ are equal upon this identification,

$$\mathcal{S}_{\mathfrak{X},\vec{Q}} = \mathcal{S}_{\mathfrak{X}_0,\vec{Q}_0},$$

as are the respective Gromov–Witten invariants,

$$F_g^{\text{top}}(\mathfrak{X}, \vec{Q}) = F_g^{\text{top}}(\mathfrak{X}_0, \vec{Q}_0).$$

Given the validity of the BKMP conjecture for the fiducial geometry,

$$F_g^{\text{top}}(\mathfrak{X}_0, \vec{Q}_0) = F_g(\mathcal{S}_{\mathfrak{X}_0,\vec{Q}_0}),$$

its validity thus follows for any toric Calabi–Yau manifold:

$$\boxed{F_g^{\text{top}}(\mathfrak{X}, \vec{Q}) = F_g(\mathcal{S}_{\mathfrak{X},\vec{Q}}).}$$

7. Conclusion

Taking our matrix model from [1] as a starting point and imposing certain minimality conditions on the spectral curve, we have thus derived the BKMP conjecture, for closed topological strings, for all toric Calabi–Yau manifolds in the large radius limit. As we have emphasized throughout, elevating our procedure to a formal proof of the conjecture requires a uniqueness result for the derivation of the spectral curve of our matrix model.

It should also be possible to extend our argument to open Gromov–Witten invariants by invoking loop operators, which relate closed to open invariants. In [8], such an operator was defined in the matrix model context. An analogous operator should also exist in the theory of Gromov–Witten invariants [48]. Establishing the equivalence of these two loop operators would allow us to conclude that the $W_n^{(g)}$'s of the spectral curve $\mathcal{S}_{\mathfrak{X}}$ are the open Gromov–Witten invariants of $\mathfrak{X}$.

Finally, our treatment of the BKMP conjecture took place at large radius. One should study the behavior of the matrix model as one moves away from large radius e.g. to orbifold points, and see whether the phase transitions of the topological string are captured accurately by the matrix model. Of course, the main tool on the topological string side employed in this work, the topological vertex, is no longer applicable in these regions of moduli space.

Acknowledgements

B.E. and O.M. would like to thank M. Bertola, J. Harnad, V. Bouchard, M. Mariño, M. Mulase, H. Ooguri, N. Orantin, B. Safnuk, for useful and fruitful discussions on this subject. A.K. would like to thank Vincent Bouchard and Ilarion Melnikov for helpful conversations. The work of B.E. is partly supported by the Enigma European network MRT-CT-2004-5652, ANR project GranMa "Grandes Matrices Aléatoires" ANR-08-BLAN-0311-01, by the European Science Foundation through the Misgam program, by the Quebec government with the FQRNT. B.E. would like to thank the AIM, as well as the organizers and all participants to the workshop [49] held at the AIM June 2009. O.M. would like to thank the CRM (Centre de recherche mathématiques de Montréal, QC, Canada) for its hospitality.

Appendix A. The Matrix Model

In this appendix, which is mainly a reprint of section 4 of [1], we present the matrix model which reproduces the topological string partition function on the fiducial geometry $\mathfrak{X}_0$, and whose spectral curve we derive in the text.

Consider the fiducial geometry $\mathfrak{X}_0$ of size $(n+1) \times (m+1)$, with Kähler parameters $t_{i,j} = g_s(a_{i,j} - a_{i,j+1}), r_{i,j} = g_s(a_{i,j+1} - a_{i+1,j})$, and $s_{i,j}$, as depicted in Fig. 1. We write

$$\vec{a}_i = (a_{0,i}, a_{1,i}, \ldots, a_{n,i}).$$

Assume that the external representations are fixed to $\vec{\alpha}_{m+1} = (\alpha_{0,m+1}, \alpha_{1,m+1}, \ldots, \alpha_{n,m+1})$ on the upper line, and $\vec{\alpha}_0 = (\alpha_{0,0}, \alpha_{1,0}, \ldots, \alpha_{n,0})$ on the lower line. For the most part, we will choose these to be trivial.

We now define the following matrix integral $\mathcal{Z}_{\mathrm{MM}}$ (MM for Matrix Model),

$$\begin{aligned}
&\mathcal{Z}_{\mathrm{MM}}(Q, g_s, \vec{\alpha}_{m+1}, \vec{\alpha}_0^T) \\
&= \Delta(X(\vec{\alpha}_{m+1}))\Delta(X(\vec{\alpha}_0)) \prod_{i=0}^{m+1} \int_{H_N(\Gamma_i)} dM_i \prod_{i=1}^{m+1} \int_{H_N(\mathbb{R}_+)} dR_i \\
&\quad \times \prod_{i=1}^{m} e^{\frac{-1}{g_s}\mathrm{tr}\left[V_{\vec{a}_i}(M_i) - V_{\vec{a}_{i-1}}(M_i)\right]} \prod_{i=1}^{m} e^{\frac{-1}{g_s}\mathrm{tr}\left[V_{\vec{a}_{i-1}}(M_{i-1}) - V_{\vec{a}_i}(M_{i-1})\right]} \\
&\quad \times \prod_{i=1}^{m+1} e^{\frac{1}{g_s}\mathrm{tr}\,(M_i - M_{i-1})R_i} \prod_{i=1}^{m} e^{(S_i + \frac{i\pi}{g_s})\mathrm{tr}\,\ln M_i} \\
&\quad \times e^{\mathrm{tr}\,\ln f_0(M_0)} e^{\mathrm{tr}\,\ln f_{m+1}(M_{m+1})} \prod_{i=1}^{m} e^{\mathrm{tr}\,\ln f_i(M_i)}. \qquad \text{(A.1)}
\end{aligned}$$

All matrices are taken of size

$$N = (n+1)d.$$

d denotes a cut-off on the size of the matrices, on which, as discussed in Sect. 5.2.1, the partition function depends only non-perturbatively. We have introduced the notation

$$\begin{aligned}
X(\vec{\alpha}_{m+1}) &= \mathrm{diag}(X(\vec{\alpha}_{m+1})_i)_{i=1,\ldots,N}, \qquad X(\vec{\alpha}_{m+1})_{jd+k} = q^{h_k(\alpha_{j,m+1})}, \\
X(\vec{\alpha}_0) &= \mathrm{diag}(X(\vec{\alpha}_0)_i)_{i=1,\ldots,N}, \qquad X(\vec{\alpha}_0)_{jd+k} = q^{h_k(\alpha_{j,0})},
\end{aligned}$$

for $k = 1, \ldots, d, j = 0, \ldots, n$, where

$$h_i(\gamma) = \gamma_i - i + d + a. \qquad \text{(A.2)}$$

$\Delta(X) = \prod_{i<j}(X_i - X_j)$ is the Vandermonde determinant. The potentials $V_{\vec{a}_i}(x)$ are given by

$$V_{\vec{a}}(X) = -g_s \sum_{j=0}^{n} \ln\left(g(q^{a_j}/X)\right) \qquad \text{(A.3)}$$

in terms of the g-functions defined as Pochhammer symbols also known as q-product or quantum Gamma-functions

$$g(x) = \prod_{n=1}^{\infty}(1 - \frac{1}{x}q^n) = (q/x; q)_\infty, \quad \Gamma_q(x) = (1-q)^{1-x}\frac{g(1)}{g(q^{1-x})}. \qquad \text{(A.4)}$$

For $i = 1, \ldots, m$, we have defined

$$f_i(x) = \prod_{j=0}^{n} \frac{g(1)^2 e^{(\frac{1}{2} + \frac{i\pi}{\ln q})\ln(xq^{1-a_{j,i}})} e^{\frac{(\ln(xq^{1-a_{j,i}}))^2}{2g_s}}}{g(xq^{1-a_{j,i}})g(q^{a_{j,i}}/x)}.$$

The denominator of these functions induces simple poles at $x = q^{a_{j,i}+l}$ for $j = 0, \ldots, n$ and $l \in \mathbb{Z}$. The numerator is chosen such that they satisfy the

relation $f_i(qx) = f_i(x)$. This enforces a simple l-dependence of the residues taken at $x = q^{a_{j,i}+l}$, given by a prefactor q^l—a fact which will be important in the following. These residues are in fact given by

$$\begin{aligned}\operatorname*{Res}_{q^{a_{j,i}+l}} f_i(x) &= q^{a_{j,i}+l}\hat{f}_{j,i} \\ &= -q^{a_{j,i}+l}\prod_{k\neq j}\frac{g(1)^2 e^{(\frac{1}{2}+\frac{i\pi}{\ln q})(1+a_{j,i}-a_{k,i})\ln q} e^{\frac{(\ln(q^{1+a_{j,i}-a_{k,i}}))^2}{2g_s}}}{g(q^{a_{j,i}-a_{k,i}})(1-q^{a_{k,i}-a_{j,i}})g(q^{a_{k,i}-a_{j,i}})},\end{aligned} \tag{A.5}$$

where $\hat{f}_{j,i}$ is independent of the integer l.

The parameters S_i are defined by

$$g_s S_i = s_{0,i-1} + t_{0,i-1} = s_{j,i-1} - \sum_{k<j} t_{k,i} + \sum_{k\leq j} t_{k,i-1}. \tag{A.6}$$

The final equality holds for arbitrary j [1].

For $i = 0$ and $i = m+1$, we define

$$\begin{aligned} f_0(x) &= \frac{1}{\prod_{j=0}^n \prod_{i=1}^d (x - q^{h_i(\alpha_{j,0})})}, \\ f_{m+1}(x) &= \frac{1}{\prod_{j=0}^n \prod_{i=1}^d (x - q^{h_i(\alpha_{j,m+1})})}. \end{aligned}$$

Notice that if the representations $\vec{\alpha}_0$ or $\vec{\alpha}_{m+1}$ are trivial, i.e. $h_i(\alpha_{j,0}) = d - i + a_{j,0}$ or $h_i(\alpha_{j,m+1}) = d - i + a_{j,m+1}$, we have

$$f_0(x) = \prod_{j=0}^n \frac{g(xq^{1-a_{j,0}-d})}{x^d g(xq^{1-a_{j,0}})}, \qquad f_{m+1}(x) = \prod_{j=0}^n \frac{g(xq^{1-a_{j,m+1}-d})}{x^d g(xq^{1-a_{j,m+1}})},$$

respectively. The functions f_0 and f_{m+1} have simple poles at $x = q^{h_l(\alpha_{j,0})}$ (resp. $x = q^{h_l(\alpha_{j,m+1})}$) for $l = 1, \ldots, d$, with residue

$$\begin{aligned} \hat{f}_{j,0;l} &= \operatorname*{Res}_{q^{h_l(\alpha_{j,0})}} f_0(x) \\ &= \frac{1}{\prod_{j'\neq j}\prod_{i=1}^d (q^{h_l(\alpha_{j,0})} - q^{h_i(\alpha_{j',0})})} \frac{1}{\prod_{i\neq l}(q^{h_l(\alpha_{j,0})} - q^{h_i(\alpha_{j,0})})}, \\ \hat{f}_{j,m+1;l} &= \operatorname*{Res}_{q^{h_l(\alpha_{j,m+1})}} f_{m+1}(x) \\ &= \frac{1}{\prod_{j'\neq j}\prod_{i=1}^d (q^{h_l(\alpha_{j,m+1})} - q^{h_i(\alpha_{j',m+1})})} \frac{1}{\prod_{i\neq l}(q^{h_l(\alpha_{j,m+1})} - q^{h_i(\alpha_{j,m+1})})}. \end{aligned}$$

The l dependence here is more intricate than above, but this will not play any role since the partitions $\alpha_{j,0}$ and $\alpha_{j,m+1}$ are kept fixed, and not summed upon.

The integration domains for the matrices R_i are $H_N(\mathbb{R}_+^N)$, i.e. the set of hermitian matrices having only positive eigenvalues. For the matrices $M_i, i =$

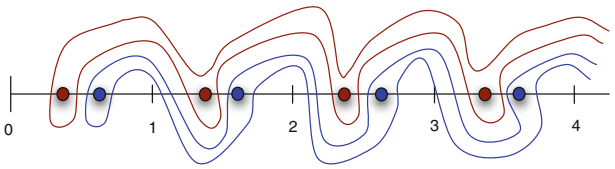

FIGURE 14. Two contours surrounding points $a+\mathbb{N}$ and $b+\mathbb{N}$, such that $a-b \notin \mathbb{Z}$

$1,\dots,m$, the integration domains are $H_N(\Gamma_i)$, where

$$\Gamma_i = \prod_{j=0}^{n} (\gamma_{j,i})^d.$$

$\gamma_{j,i}$ is defined as a contour which encloses all points of the form $q^{a_{j,i}+\mathbb{N}}$, and does not intersect any contours $\gamma_{k,l}, (j,i) \neq (k,l)$. For this to be possible, we must require that the differences $a_{j,i} - a_{j',i'}$ be non-integer. The normalized logarithms of two such contours are depicted in Fig. 14.

We have defined

$$H_N(\Gamma_i) = \{M = U\Lambda U^\dagger, \quad U \in U(N), \Lambda = \mathrm{diag}(\lambda_1,\dots,\lambda_N) \in \Gamma_i\},$$

i.e. $H_N(\Gamma_i)$ is the set of normal matrices with eigenvalues on Γ_i. By definition, the measure on $H_N(\Gamma_i)$ is (see [33])

$$dM = \frac{1}{N!}\Delta(\Lambda)^2 dU d\Lambda, \tag{A.7}$$

where dU is the Haar measure on $U(N)$, and $d\Lambda$ is the product of the measures for each eigenvalue along its integration path.

The integration domains for the matrices M_0, M_{m+1} are $H_N(\Gamma_0)$, $H_N(\Gamma_{m+1})$, respectively, where

$$\Gamma_0 = \left(\sum_{j=0}^{n} \gamma_{j,0}\right)^N, \qquad \Gamma_{m+1} = \left(\sum_{j=0}^{n} \gamma_{j,m+1}\right)^N. \tag{A.8}$$

Appendix B. Transition to Fiducial Geometry

In this appendix, we provide an algorithm to obtain a fiducial geometry from any member of the class of toric geometries we are considering, built from the triangulation of a finite connected convex lattice polygon in $\mathbb{Z}^2$.

To begin, add vertices such that the polygon is embedded in a rectangle. By further triangulating if necessary, the rectangle can always be triangulated by minimal faces. Label the lowest left vertex by (0,0), and the highest right vertex by $(M+1, N+1)$. Set $m = n = 0$. An **EtoN** edge (read 'east to north') in the following will signify an edge forming an angle between 0 and $\pi/2$ from the horizontal.

Routine: Consider the vertex (m, n). It is necessarily connected to $(m + 1, n)$ and $(m, n + 1)$.

- If these are the only two EtoN edges emanating from (m, n), and
  - if $m < M$, increase m by 1. If the vertices $(m+1, n)$ and $(m-1, n+1)$ are connected by an edge, flop this edge. Rerun the **routine**.
  - Else, if $n < N$, set $m = 0$, increase n by 1 and rerun the **routine**. Else, the algorithm is complete.
- **Subroutine:** If there is an EtoN edge emanating from (m, n)—other than the one connecting to (0,1)—below the diagonal, consider the lowest lying such edge. It forms the diagonal of a parallelogram. Flop it. Repeat this **subroutine** till the opening condition is no longer met.
- **Subroutine:** If there is an EtoN edge emanating from (m, n)—other than the one connecting to (1,0)—above the diagonal, consider the highest lying such edge. It forms the diagonal of a parallelogram. Flop it. Repeat this **subroutine** till the opening condition is no longer met.
- There are three EtoN edges emanating from (m, n). Flop the diagonal edge connecting to $(m + 1, n + 1)$. If $m < M$, increase m by 1 and rerun the **routine**. Else, if $n < N$, set $m = 0$, increase n by 1 and rerun the **routine**. Else, the algorithm is complete.

References

[1] Eynard, B., Kashani-Poor, A.-K., and Marchal, O.: A matrix model for the topological string I: Deriving the matrix model. arXiv:1003.1737 [hep-th]

[2] Eynard, B.: Master loop equations, free energy and correlations for the chain of matrices. JHEP **11**, 018 (2003), arXiv:hep-th/0309036

[3] Eynard, B., Ferrer, A.P.: Topological expansion of the chain of matrices. JHEP **07**, 096 (2009)

[4] Migdal, A.A.: Loop equations and 1/N expansion. Phys. Rep. **102**(4), 199–290 (1983)

[5] Ambjorn, J., Chekhov, L., Kristjansen, C. F., Makeenko, Y.: Matrix model calculations beyond the spherical limit. Nucl. Phys. **B404**, 127–172 (1993), arXiv:hep-th/9302014

[6] Eynard, B.: Topological expansion for the 1-hermitian matrix model correlation functions. JHEP **11**, 031 (2004), arXiv:hep-th/0407261

[7] Alexandrov, A.S., Mironov, A., Morozov, A.: Solving Virasoro constraints in matrix models. Fortsch. Phys. **53**, 512–521 (2005), arXiv:hep-th/0412205

[8] Eynard, B., Orantin, N.: Invariants of algebraic curves and topological expansion. arXiv:math-ph/0702045

[9] Chekhov, L., Marshakov, A., Mironov, A., Vasiliev, D.: DV and WDVV. Phys. Lett. **B562**, 323–338 (2003), arXiv:hep-th/0301071

[10] Eynard, B., Marino, M., Orantin, N.: Holomorphic anomaly and matrix models. JHEP **06**, 058 (2007), arXiv:hep-th/0702110

[11] Eynard, B.: Recursion between Mumford volumes of moduli spaces. arXiv: 0706.4403

[12] Witten, E.: Chern-Simons gauge theory as a string theory. Prog. Math. **133**, 637–678 (1995), arXiv:hep-th/9207094

[13] Marino, M.: Chern-Simons theory, matrix integrals, and perturbative three-manifold invariants. Commun. Math. Phys. **253**, 25–49 (2004), arXiv:hep-th/0207096

[14] Marino, M.: Chern–Simons theory, matrix models, and topological strings. pp. 197 Clarendon, Oxford (2005)

[15] Bouchard, V., Klemm, A., Marino, M., Pasquetti, S.: Remodeling the B-model. Commun. Math. Phys. **287**, 117–178 (2009), arXiv:0709.1453 [hep-th]

[16] Marino, M.: Open string amplitudes and large order behavior in topological string theory. JHEP **03**, 060 (2008), arXiv:hep-th/0612127

[17] Bouchard, V., Marino, M.: Hurwitz numbers, matrix models and enumerative geometry. arXiv:0709.1458 [math.AG]

[18] Dijkgraaf, R., Vafa, C.: Two Dimensional Kodaira–Spencer Theory and Three Dimensional Chern–Simons Gravity. http://arxiv.org/abs/0711.1932

[19] Orantin, N.: Symplectic invariants, Virasoro constraints and Givental decomposition. arXiv:0808.0635 [math-ph]

[20] Klemm, A., Sulkowski, P.: Seiberg–Witten theory and matrix models. Nucl. Phys. **B819**, 400–430 (2009), arXiv:0810.4944 [hep-th]

[21] Sulkowski, P.: Matrix models for 2* theories. arXiv:0904.3064 [hep-th]

[22] Borot, G., Eynard, B., Mulase, M., Safnuk, B.: A matrix model for simple Hurwitz numbers, and topological recursion. arXiv:0906.1206 [math-ph]

[23] Eynard, B., Mulase, M., Safnuk, B.: The Laplace transform of the cut-and-join equation and the Bouchard–Marino conjecture on Hurwitz numbers. arXiv:0907.5224 [math.AG]

[24] Chen, L.: Bouchard–Klemm–Marino–Pasquetti Conjecture for $\mathbb{C}^3$. (2009), arXiv:0910.3739 [math.AG]

[25] Zhou, J.: Local Mirror Symmetry for One-Legged Topological Vertex. (2009), arXiv:0910.4320 [math.AG]

[26] Ooguri, H., Sulkowski, P., Yamazaki, M.: Wall Crossing as Seen by Matrix Models. arXiv:1005.1293 [hep-th]

[27] Di Francesco, P., Ginsparg, P.H., Zinn-Justin, J.: 2-D Gravity and random matrices. Phys. Rept. **254**, 1–133 (1995), arXiv:hep-th/9306153

[28] Hori, K., Vafa, C.: Mirror symmetry. arXiv:hep-th/0002222

[29] Aganagic, M., Klemm, A., and Vafa, C.: Disk instantons, mirror symmetry and the duality web. Z. Naturforsch. **A57**, 1–28 (2002), arXiv:hep-th/0105045

[30] Katz, S.H., Klemm, A., Vafa, C.: Geometric engineering of quantum field theories. Nucl. Phys. **B497**, 173–195 (1997), arXiv:hep-th/9609239

[31] Aganagic, M., Klemm, A., Marino, M.,Vafa, C.: The topological vertex. Commun. Math. Phys. **254**, 425–478 (2005), arXiv:hep-th/0305132

[32] Iqbal, A., Kashani-Poor, A.-K.: The vertex on a strip. Adv. Theor. Math. Phys. **10**, 317–343 (2006), arXiv:hep-th/0410174

[33] Mehta M.L. (2004) Random matrices. In: Pure and Applied Mathematics (Amsterdam), vol. 142, 3rd edn. Elsevier, Amsterdam

[34] Di Francesco, P., Ginsparg, P. H., Zinn-Justin, J.: 2-D Gravity and random matrices. Phys. Rept. **254**, 1–133 (1995), arXiv:hep-th/9306153

[35] Bertola M. (2007) Biorthogonal polynomials for 2-matrix models with semiclassical potentials. J. Approx. Theory **144**, 162

[36] Eynard, B., Orantin, N.: Algebraic methods in random matrices and enumerative geometry. arXiv:0811.3531 [math-ph]

[37] Bonnet, G., David, F., Eynard, B.: Breakdown of universality in multi-cut matrix models. J. Phys. **A33**, 6739–6768 (2000), arXiv:cond-mat/0003324

[38] Eynard, B.: Loop equations for the semiclassical 2-matrix model with hard edges. J. Stat. Mech. **0510**, P006 (2005), arXiv:math-ph/0504002

[39] Chekhov, L.: Matrix models with hard walls: Geometry and solutions. J. Phys. A **39**, 8857–8894 (2006), arXiv:0602013 [hep-th]

[40] Prats Ferrer, A.: New recursive residue formulas for the topological expansion of the Cauchy Matrix Model. JHEP **10**, 090 (2010)

[41] Fay, J.D.: Theta functions on Riemann surfaces. Lecture Notes in Mathematics, vol. 352. Springer, Berlin (1973)

[42] Kokotov, A., Korotkin, D.: Tau-function on Hurwitz spaces. Math. Phys. Anal. Geom. **7**, 47–96 (2004)

[43] Eynard, B., Kokotov, A., Korotkin, D.: Genus one contribution to free energy in hermitian two- matrix model. Nucl. Phys. **B694**, 443–472 (2004), arXiv:hep-th/0403072

[44] Johansson, K.: The arctic circle boundary and the Airy process. Ann. Probab. **33**(1), 1–30 (2005)

[45] Jost, J.: Compact Riemann surfaces. In: An introduction to contemporary mathematics, 2nd edn. Springer, Berlin (2002)

[46] Witten, E.: Phases of $N = 2$ theories in two dimensions. Nucl. Phys. **B403** 159–222 (1993), arXiv:hep-th/9301042

[47] Konishi, Y., Minabe, S.: Flop invariance of the topological vertex. Int. J. Math. **19**, 27–45 (2008), arXiv:math/0601352

[48] Cavalieri, R.: Private communications.

[49] *Recursion structures in topological string theory and enumerative geometry.* June 8 to June 12, 2009, at the American Institute of Mathematics (AIM), Palo Alto, California

Bertrand Eynard and Olivier Marchal
Institut de Physique Théorique
CEA, IPhT
91191 Gif-sur-Yvette, France
e-mail: `bertrand.eynard@cea.fr;`
`olivier.marchal2@yahoo.fr`

and

CNRS, URA 2306
91191 Gif-sur-Yvette, France

Amir-Kian Kashani-Poor
Institut des Hautes Études Scientifiques
Le Bois-Marie
35, route de Chartres
91440 Bures-sur-Yvette, France

and

Laboratoire de Physique Théorique de l'École Normale Supérieure
24, rue Lhomond
75231 Paris, France
e-mail: kashani@lpt.ens.fr

Olivier Marchal
Centre de recherches mathématiques
Université de Montréal
C.P. 6128, Succ. centre-ville, Montreal
QC H3C 3J7, Canada

Communicated by Marcos Marino.

Received: June 6, 2011.

Accepted: March 9, 2012.